1

Stille Polycondensation: A Versatile Synthetic Approach to Functional Polymers

Tianyue Zheng, Alexander M. Schneider, and Luping Yu

1.1 Introduction

The development of functional polymers is a very active research field that covers every aspects of our lives and has had huge impact on human society due to their applications in many cutting-edge technologies, such as energy conversion and storage, electronic devices, biotechnology, and health care, to name a few [1]. Scientists from different disciplines have invented numerous new materials for those purposes. Integral to these efforts is the development of efficient, versatile, and scalable synthesis techniques, which in turn enable the development of new functional materials. Thus, new synthetic methodologies are always a critical research topic that is actively pursued. A large number of recent advances can be cited to support this view, such as ring-opening metathesis polymerization (ROMP), atom transfer radical polymerization (ATRP, a type of "living" radical polymerization), and controlled Ziegler–Natta polymerization [2, 3]. Most recently, polycondensations based on transition metal-catalyzed CC bond formation reactions have emerged as important methodologies for synthesis of electro-optic materials containing large systems. These reactions include Stille, Suzuki, Negishi, Heck, and so on [4–7]. The Stille reaction is one of the best methods for the synthesis of organic functional materials due to its excellent compatibility with various functional groups and high reaction yield.

The most attractive application of the Stille coupling reaction is in the synthesis of conjugated, polyaromatic semiconducting materials, which are an important class of materials for organic electronics. These materials exhibit good solubility in various solvents, which allows them to be fabricated into devices using inexpensive solution-phase printing techniques [8]. Over the past several decades, the development of semiconducting polymers has led to the advent of new technologies for numerous applications, ranging from organic light-emitting diodes (OLEDs), field effect transistor (FET), and organic photovoltaic (OPV) solar cells [7]. Among these semiconducting polymers, the majority of them, especially those containing thiophene moieties, can be synthesized via Stille polycondensation from-related monomers. These polymers bear a wide variety of functional groups and their emergence is enabled by the power and broad scope of the

Stille polycondensation. This chapter summarizes recent progress in investigating the Stille polycondensation and its application to the development of functional materials.
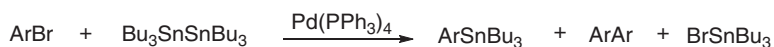
1.1.1 History of the Stille Reaction (and Polycondensation)

The Stille coupling reaction refers to the reaction between an organostannane (also called *organotin*) and an organic electrophile in the presence of palladium catalyst to generate new C–C single bond (Scheme 1.1) .
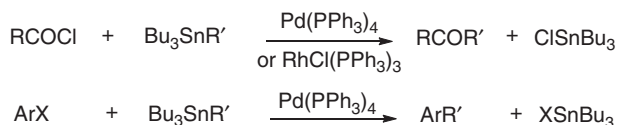
$$R_1-X \quad + \quad R_2-Sn- \quad \xrightarrow{[Pd(0)]} \quad R_1-R_2 \quad + \quad X-Sn-$$
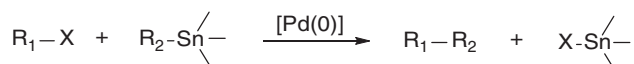
Scheme 1.1 The Stille coupling reaction scheme.

In 1976, Eaborn reported a Pd-catalyzed reaction using bis(tributyltin) to prepare aryltin compounds, where C–Sn bonds were formed (Scheme 1.2) [9]. Later, in 1977, Kosugi used a similar method to report the first C–C bond formation from cross-coupling between acyl chlorides or aryl halides and organostannanes (Scheme 1.3) [10–12]. These disclosures were considered the first examples of cross-coupling reactions between organostannanes and electrophilic partners.

$$ArBr \quad + \quad Bu_3SnSnBu_3 \quad \xrightarrow{Pd(PPh_3)_4} \quad ArSnBu_3 \quad + \quad ArAr \quad + \quad BrSnBu_3$$

Scheme 1.2 Synthesis of aryltin compounds by Eaborn *et al.* [9].

$$RCOCl \quad + \quad Bu_3SnR' \quad \xrightarrow[\text{or RhCl(PPh}_3)_3]{Pd(PPh_3)_4} \quad RCOR' \quad + \quad ClSnBu_3$$

$$ArX \quad + \quad Bu_3SnR' \quad \xrightarrow{Pd(PPh_3)_4} \quad ArR' \quad + \quad XSnBu_3$$

Scheme 1.3 Coupling of halides and organostannanes by Kosugi *et al.* [10–12].

Following these examples, John K. Stille carried out extensive studies on the reaction scope and mechanism beginning in 1978. The original report from Stille and coworkers involved the synthesis of ketones from acyl chlorides and organostannanes [13]. Following that, the general features of this reaction were revealed and it quickly became a standard method in organic synthesis and one of the most useful procedures for carbon–carbon bond formation, especially of sp^2-sp^2 C–C bonds. His major body of work was summarized in a very influential review in 1986 [13–15]. Together with the Suzuki reaction, a palladium-catalyzed cross-coupling of organoboranes and electrophiles, the Stille reaction is one of the most efficient methods for preparing functional materials, especially those containing extended conjugation systems that are linked by sp^2-sp^2 C–C bonds.

By incorporating a ditin compound and a difunctional electrophile, the Stille reaction was used to synthesize polymers as early as the 1980s and the early 1990s, when polycondensation between organo-ditin monomers and dihalide monomers was developed [7]. Yu and coworkers further developed this methodology, including reaction scope and

conditions, for making high molecular weight heteroaromatic diblock copolymers in the early 1990s (Schemes 1.4 and 1.5) [16–18].

Scheme 1.4 Synthesis of PPT by Stille polycondensation [16, 17].

Scheme 1.5 Synthesis of PPTs with metalloporphyrin or pendent carbazole units [18].

1.2 Reaction Mechanism

1.2.1 Simplified Mechanism

The Stille reaction is a Pd(0)-catalyzed cross-coupling reaction. The active Pd(0) species may be generated from Pd(II) precursor that is reduced by the organostannane before entering the catalytic cycle. In his review article in 1986 [15], Stille proposed the reaction mechanism based on the study of coupling between benzoyl chloride and tributyl(phenyl)stannane with $Pd(Bn)Cl(PPh_3)_2$ ($PPh_3 =$ triphenylphosphine) as the catalyst. The proposed mechanism is similar to other Pd(0)-mediated cross-coupling reactions, in which the PdL_2 (L = PPh_3) complex was assumed to be the active catalytic species. The PdL_2 undergoes oxidative addition with organic electrophile $R^1 - X$ to form

R^1PdL_2X, which then undergoes a slow transmetallation with organostannane R^2SnMe_3 to form $R^1PdL_2R^2$, followed by a reductive elimination step to give the product R^1-R^2 and regenerate the PdL_2 active species. A general feature of this mechanism is that a *trans−cis* isomerization step is needed for the ensued reductive elimination. Though this mechanism (Scheme 1.6) was generally accepted by the research community, more extensive investigation revealed more complexity of the mechanism. Espinet and coworkers have written in-depth reviews of the mechanistic study of the Stille reaction in 2004 [19] and most recently in 2015 [20]. It was shown that the actual mechanism may vary according to different reaction conditions, including catalyst, ligands, solvents, and additives. There is no simple answer to the actual mechanism and thus is referred as the *mechanistic black box* [19]. In the three major steps of the mechanism, the oxidative addition and reductive elimination steps are extensively studied and relatively well understood, but the transmetallation step is more complicated and not well understood.
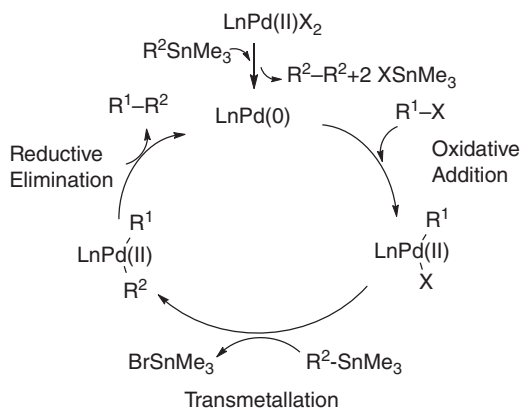
**Scheme 1.6** A simplified mechanism for Stille coupling [7, 19].

For halides with a $C(sp^3)-X$ bond, the oxidative addition of $R-X$ to $Pd(0)$ is usually a bimolecular reaction (S_N2) and the configuration of product will be affected by the choice of different solvents. For $C(sp^2)-X$, this step is considered to go through a three-center transition state between the electrophile $R-X$ and the active $Pd(0)L_2$ (L = ligand) to give a kinetic product of *cis*-[$Pd(II)RXL_2$] complex, which can isomerize to the more thermodynamically stable *trans*-[$PdRXL_2$] complex [19]. This *cis*-to *trans*-isomerization is usually fast; very often only the *trans*-complex is found. However, with bidentate ligands to stabilize the intermediate, the *cis* complex may be observed (Scheme 1.7). For example, in the reaction of ArOTf (Ar = C_6F_5, $C_6Cl_2F_3$) and $RSnBu_3$ (R = vinyl), Espinet and coworkers were able to observe the *cis* complexes [(dppe)Pd(Ar)(OTf)] (dppe = 1,2-bis(diphenylphosphino)ethane), which were stable in the solid state and fully characterized by nuclear magnetic resonance (NMR) spectroscopies [21]. Milstein and coworkers studied the mechanism of the oxidative addition of chlorobenzene to $Pd(dippp)_2$ (dippp = 1,3-bis(diisopropylphosphanyl)propane) in dioxane [22]. They monitored the intermediates by ^{31}P NMR and found that the *cis*-(dippp)Pd(Ph)Cl and *trans*-(η^1-dippp)$_2$Pd(Ph)Cl are formed in parallel pathways.

While in equilibrium with each other, the *cis*-complex is favored both kinetically and thermodynamically.
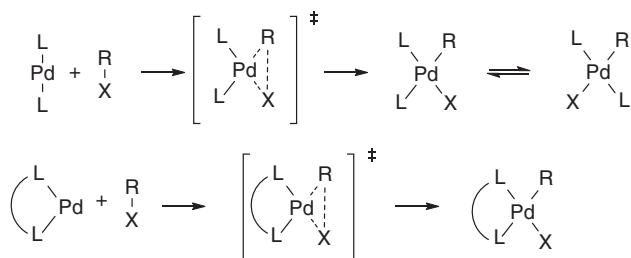
Scheme 1.7 Formation of *cis* complex and *cis–trans* isomerization [19]. L = ligand. (Adapted with permission from [19]. Copyright 2004 WILEY-VCH Verlag GmbH & Co. KGaA, Weinheim.)

The major difference between the Stille reaction and other similar Pd-catalyzed cross-coupling reactions is in the transmetallation step. During the transmetallation step, the organostannanes interact with the Pd center, resulting in Sn–C bond cleavage and Pd–C bond formation. Unlike in other modern Pd-catalyzed coupling reactions, the nature of the Sn–C bond is neither as strong nor as polar as other metal–carbon bonds, such as B–C, Zn–C, and Mg–C bonds. Espinet and Echavarren point out that the transmetallation step in the Stille reaction involves the electrophilic cleavage of Sn–C bond (S_E2) by the Pd(II) complex (from oxidative addition), which could also be viewed as a ligand substitution (S_N2) on the Pd(II) complex [19]. These complexes are usually 16-electron, square planar, tetracoordinated, and can experience ligand substitution via two possible pathways. One pathway is dissociative, which would involve a 14-electron, T-shaped intermediate with substitution being determined by the ligand with the highest *trans* influence that weakens the bond *trans* to it. The other is associative, which would involve an 18-electron, trigonal bipyramidal intermediate with substitution being determined by the ligand with the highest *trans* effect that leads the lowest energy transition state [23]. The solvent could play a role in this step, by assisting the ligand substitution or serving as ligand itself, such as THF or DMF [24, 25]. For the intermediate in the electrophilic cleavage process, both an open and cyclic (Scheme 1.8) transition states are possibilities, which have been proposed to explain this (S_E2) step. Stille considered this step to involve an open transition state from his studies on the [Pd(Bn)Cl(PPh$_3$)$_2$]-catalyzed coupling of benzoyl chloride with (S)-PhCHDSnBu3 [15, 28], which explains the fact that the transmetallation step can be very fast and that the inversion configuration of the alpha carbon sometimes occurs. Espinet and coworkers also reported an open transition state in the coupling of organotriflates, again using triphenylarsine (AsPh$_3$) as ligand [26]. However, with the same ligand but organohalide substrate, Espinet and coworkers reported that the *trans* complex reacts with organostannane through a cyclic transition state with release of ligand [27], which explains the inverse dependence on the concentration of ligand on the reaction rate [15, 23]. All of these findings demonstrate the complexity of the transmetallation step, which may go through different pathways according to different reaction conditions.
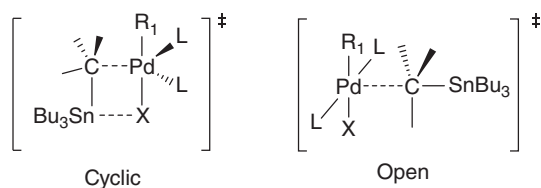
Scheme 1.8 Cyclic and open transition states [26, 27].

Reductive elimination leads to formation of the final product and regenerates the active Pd(0) species into the catalytic cycle. Before the formation of the coupled product from the transmetallation intermediate, a *trans-* to *cis*-isomerization places the coupling partners in *cis*-position to each other [15]. A three-coordinate, T-shaped 14-electron complex resulting from ligand dissociation has also been proposed to be the intermediate [15, 19, 23]. For example, Hartwig and coworkers reported the formation of 14-electron ArPdXL (L = PPh$_3$) complexes by dissociation of one ligand L from 16-electron *trans*-ArPdXL$_2$ complexes (Scheme 1.9) [29]. The ArPdXL complexes then react with organostannane to generate the ArPdRL complexes, which then undergo a fast reductive elimination to produce the Ar-R product. The rate of the reductive elimination step is usually fast, but might be slow when allyl groups or chelating ligands are involved [30].


L = phosphine   Ar = *p*-Tol, R = Ph, SAr, StBu   R′ = Me, Bu
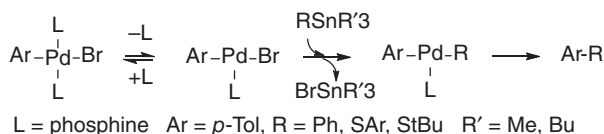
Scheme 1.9 A ligand dissociation to form a T-shaped complex [29].

Taking this knowledge together, a more complicated mechanism has been proposed by Espinet and coworkers (Scheme 1.10) [20]. In this mechanism, in addition to the regular three major steps, more details about the configuration of intermediate species have been added, taking into account the effect of ligands, solvents, and so on. This more detailed mechanism may give clues to the nature of side reactions, which could affect the structure of resulting polymers. A more detailed understanding of reaction mechanism under proper conditions is crucial to synthesize high-quality polymers. This point will be further illustrated in the later section of this chapter.

1.3 Reaction Conditions

The Stille polycondensation reaction involves two types of monomers, an organodihalide (or organoditriflate) and an organodistannane. Typically, diiodo monomers are more reactive than dibromo compounds, and dichlorides are the least reactive primarily due to their low reactivity in the oxidative addition step. However, while organochlorides can be activated in the synthesis of small molecules by using special catalyst systems [31, 32], the examples of using chlorides to synthesize polymers are rare. In general, it has been found that the combination of electron-rich organotin compounds and
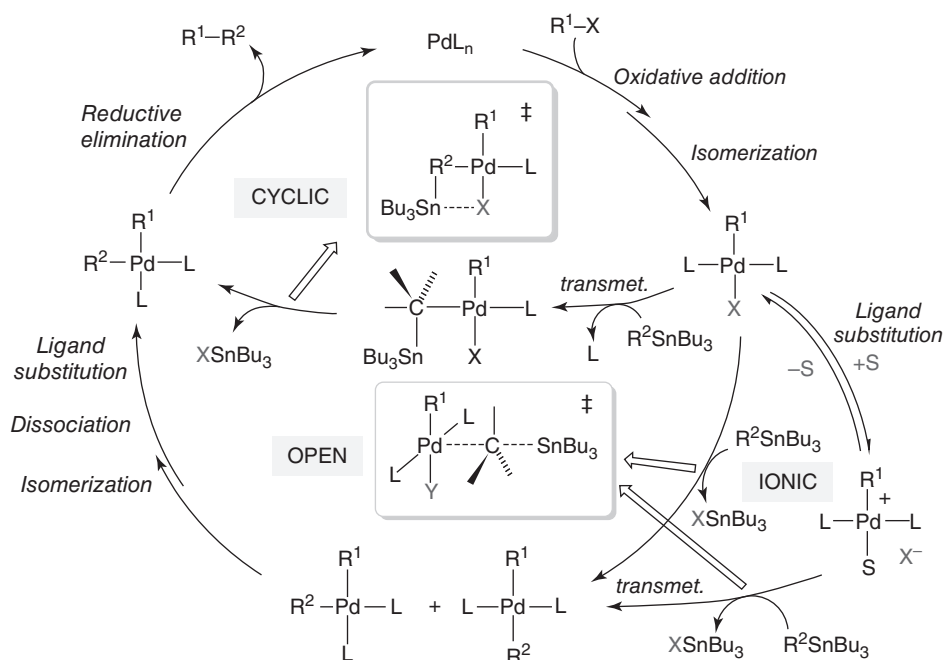
Scheme 1.10 A more complex mechanism by Espinet *et al.* [20]. (Reprinted with permission from [20]. Copyright 2015 American Chemical Society.)

electron-deficient halide or triflate is beneficial for the synthesis of polymers exhibiting high molecular weight, as the electron-withdrawing groups may facilitate the oxidative addition step and the electron-rich organostannane favors the transmetallation step [7, 18].

1.3.1 Catalyst and Ligand

There are many palladium compounds that provide catalytic centers for the Stille reaction, including Pd(II) sources such as dichlorobis(triphenylphosphine)-palladium(II) [$PdCl_2(PPh_3)_2$] and palladium(II) acetate [$Pd(OAc)_2$] and Pd(0) sources such as tetrakis(triphenylphosphine)palladium(0) [$Pd(PPh_3)_4$] and tris(dibenzylideneacetonyl) dipalladium(0) [$Pd_2(dba)_3$]. However, since the active species in the catalytic cycle is Pd(0) complex, a reducing agent will be needed if Pd(II) is added as the Pd source. For example, adding PPh_3 to $Pd(OAc)_2$ rapidly leads to the formation of [$Pd(OAc)_2(PPh_3)_2$] complex, which undergoes slow intramolecular reduction to form a Pd(0) complex [33]. $Pd(PPh_3)_4$ and $Pd_2(dba)_3$ are the most frequently used, commercially available Pd catalysts for the Stille coupling, particularly for polymerization. $Pd(PPh_3)_4$ is reactive but is not stable against air or moisture, since the free PPh_3 can be easily oxidized by air to form triphenylphosphine oxide ($OPPh_3$), accordingly, $Pd_2(dba)_3$ is a more air-stable compound [7].

In addition to catalyst, the selection of ligand is also important in developing a robust catalytic system. Size and bulkiness, as well as electron-donating ability are some key parameters for ligands applied in the Stille reaction, in which phosphine ligands are the

most commonly used ligands. For example, Yu and coworkers examined the reaction scope and conditions of Stille coupling for making high molecular weight conjugated copolymers [18]. It was found that catalyst concentration, different solvents and ligands, and structures of monomers could largely affect the polymerization. If a Pd(II) catalyst is used, a stoichiometric excess of the distannyl monomer is necessary to generate the Pd(0) complex and enhance the molecular weight of the resulting polymer. When different ligands are used, they also found that the molecular weight and dispersity of resulting polymers showed a trend as $AsPh_3 > P(2\text{-furyl})_3 > PPh_3$, indicating the reactivity of ligands.

Though they suffer from sensitivity to trace amounts of oxygen and moisture, the bulky electron-rich phosphine ligands are widely used in the Stille coupling reaction to extend the reaction scope to weakly active organotin and electrophile (**4−7**, Scheme 1.11) [34−37]. For example, proazaphosphatrane ligands (**6**) are very effective for enabling the coupling of aryl chlorides with a variety of organostannanes, including sterically hindered ones [36]. Fu and coworkers studied the bulky ligand $P(t\text{-Bu})_3$ (**7**), leading to the first effective Stille couplings of unactivated aryl chlorides with organostannanes [37]. This catalyst system was found to be highly effective; highly hindered tetrasubstituted biaryls may be produced, and the reaction can take place at room temperature in some cases. They also found the unexpected selectivity of Ar-Cl over Ar-OTf in the reaction involving ArCl/ArOTf or ClC_6H_4OTf when $P(t\text{-Bu})_3$ was used (Scheme 1.12).
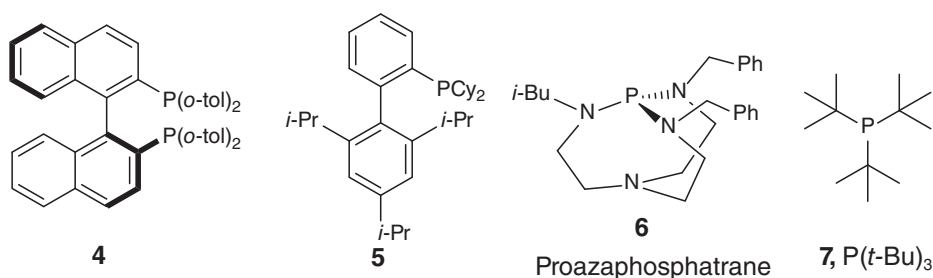

Scheme 1.11 The structure of some bulky phosphine ligands [34−37].
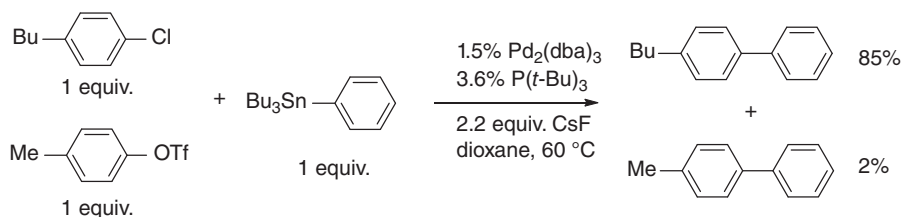
Scheme 1.12 Selectivity of ArCl over ArOTf in Stille coupling [37].

In fact, bulky phosphine ligands can assist every step in the catalytic cycle of the Stille reaction, as concluded by Espinet and coworkers in 2015 (Scheme 1.13) [20]. This is shown to be due to the stabilization of monoligated Pd intermediates due to the bulk

of the phosphine ligand. At the oxidative addition step, the monoligated Pd(0) species facilitates nucleophilic attack at the Ar–X bond from the ligand free side; while the electron richness of the phosphine provides efficient electron back-donation to the σ^* Ar–X orbital, making the oxidative addition possible even for Ar–X bond with very low nucleophilicity. At the transmetallation step, a three-centered, 14-electron Pd(II) complex is stabilized by the ligand, beneficial for the nucleophilic attack by the organostannane, the Sn–C bond of which is of low polarity. Moreover, there is no need for *trans-* to *cis*-isomerization as in the case of a tetracoordinated Pd(II) complex, further inducing reductive elimination.

Oxidative addition   Transmetallation   Reductive elimination
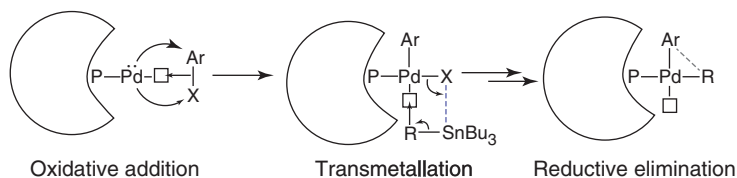
Scheme 1.13 Bulky ligands assist Stille coupling [20]. (Reprinted with permission from [20]. Copyright 2015 American Chemical Society.)

Another factor that is of no less importance is the electronic effect of the ligands. For example, the reduction of $[Pd(OAc)_2(PPh_3)_2]$ to Pd(0) complex will be enhanced by electron-withdrawing groups at the para position of the aryl groups on the phosphine [33]. $[Pd(dba)(AsPh_3)_2]$ was found to be more stable than analogous phosphine complexes $[Pd(dba)L_2]$ (L = PPh_3 or tri(2-furyl)phosphine (TFP)) due to its better electron-donating ability [38]. Farina and coworkers carried out a kinetic study of ligands with different donicities [39]. The coupling was between a model reaction system of iodobenzene and vinyltributyltin with $Pd_2(dba)_3$ as the palladium source, and the ligands studied were PPh_3, tri(*p*-anisyl)phosphine (TAP), TFP, and $AsPh_3$. It was shown that the coupling rate when using TFP and $AsPh_3$ is three and four orders of magnitude faster, respectively, than that of PPh_3. They rationalized this by the observed inhibitory effect on the cross-coupling of "strong" ligands, such as both PPh_3 and TAP. Stronger electron-donating ligands are also more easily oxidized, leading to formation of palladium black, deactivating the catalyst [7].

Since the pathways in the Stille coupling reaction may be influenced by the reaction conditions, it is crucial to carefully optimize the conditions in order to obtain desired products. For the Stille polycondensation, the reaction conditions are even more critical because in addition to high yield (thus high degree of polymerization), molecular weight distribution (characterized by dispersity) is important in controlling the quality of the resulting polymers. Selection of the correct set of conditions for Stille polycondensation is often a trial-and-error process when different monomer combinations are used [7]. The optimized catalytic systems for Stille polycondensation to achieve high-quality polymers may vary according to different target polymers.

1.3.2 Solvent

The solvent lays the foundation for the complex system of reaction conditions, which involves the interplay of many factors including catalyst, ligand, and additives, in addition to the solvent. The commonly used solvents for the Stille reaction include benzene,

toluene, xylene, tetrahydrofuran (THF), dimethylfluoride (DMF), *N*-methylpyrrolidone (NMP), dioxane, and chloroform. They show a wide range of polarity, as well as solubility toward organic molecules. Choosing the appropriate solvent is critical for the reaction to be efficient, since the solvent not only solubilizes the organic reagents and intermediates, but also takes part in the catalytic cycle by serving as ligand to Pd catalyst or assisting in ligand dissociation. For example, Amatore and coworkers [25] studied the coupling of PhI with tributyl(vinyl)tin in DMF with $[Pd(dba)(AsPh_3)_2]$ as the catalyst, and found that the transmetallation takes place in the solvent-coordinated *trans*-$[PdPhI(AsPh_3)(DMF)]$ complex. Moreover, the solvent is found to affect the configuration (retention or inversion) of final product based on its polarity and coordinating ability [40, 41].

For polymerization, the demand of the solvent is even greater than those in small-molecule Stille coupling. Like in the small-molecule reaction, the solvent should dissolve the starting monomers, stabilize the catalyst, and maintain catalytic ability; for Stille polymerization, the solvent must also keep the growing polymer chain in solution as long as possible in order to obtain polymers with high molecular weight and narrow dispersity. For example, DMF is highly polar and can coordinate to the catalyst center as ligand; however, many polymers, especially conjugated polymers used in functional materials, show low solubility in DMF. On the contrary, polymers show good solubility in toluene, which is less polar and coordinating. Yu and coworkers found that mixed solvents such as toluene/DMF (typically in a 4 : 1 ratio) can provide benefits of each individual solvent while avoiding the disadvantages, enabling a good yield of high molecular weight polymers [18]. In addition, high-boiling solvents are always used for polymerization procedures, which often require high temperature to facilitate the polymerization reaction and increase the solubility of final polymers. As a result, toluene (b.p. = 110 °C) and chlorobenzene (b.p. = 131 °C) are often used in polymerization reactions. For example, Yan and coworkers used chlorobenzene as solvent to carry out the Stille polycondensation either in a conventional or a microwave-assisted conditions, with the reaction temperature reaching over 150 °C in the latter case [42].

1.3.3 Additive

The additives used in the Stille coupling are usually inorganic salts, such as LiCl, CsF, and CuI. The active species may be either anion or cation; the role additives play in the catalytic cycle can be varied according to different combinations of other reaction conditions, such as ligand and solvent.

LiCl is a common additive in the Stille coupling since the very early stages of this methodology. Prof. Stille found that LiCl could accelerate the coupling of organostannanes with vinyl and aryl triflates [43]. LiCl was proposed to transform the triflato complex into the more reactive chloro complex, which then enters the catalytic cycle as with other organic halides. Similar effects have been found with iodide and bromide salts as well [44, 45]. However, Farina and coworkers reported that the effect of LiCl additive was largely dependent on the reaction conditions, leading to both accelerating and retarding effects [39, 46]. For example, in the coupling of vinyl triflate and aryl tributylstanne with $Pd_2(dba)_3$ as the catalyst in NMP, LiCl was found to retard the reaction when TFP or PPh_3 was used as ligand, but accelerate the reaction for $AsPh_3$. Interestingly, they found that the accelerating effect was extremely significant when no additional ligand was added. Espinet and coworkers have also reported both positive and negative effects

of LiCl [26]. LiCl favors the coupling of C_6F_5I with organostannanes when catalyzed by $[Pd(AsPh_3)_4]$ in THF, by promoting the oxidative addition step. By contrast, with the more nucleophilic $[Pd(PPh_3)_4]$, LiCl retards the reaction since the oxidative addition has already taken place without LiCl.

Some Lewis bases have been reported to facilitate Stille coupling by activating the organostannane. The most widely studied are fluoride salts, such as CsF, KF, and Bu_4NF, which can activate the tin compounds due to its fluorophilicity. It is suggested that a pentavalent tin complex with enhanced reactivity toward transmetallation be formed by the coordination of F^- anion to tin compounds [7]. Fu and coworkers used CsF to activate the organostannane, enabling its coupling with aryl chlorides, and particularly with aryl bromides at room temperature, in their $Pd/P(t\text{-}Bu)_3$ catalytic system [37]. Examples of applying other Lewis bases have also been reported. Besides fluoride salts, Fu and coworkers have studied the activating effect of bases such as Cs_2CO_3, NaOH, NaOMe, $N(i\text{-}Pr)_2Et$, and others in assisting the Stille coupling reaction [47]. In addition, amines can also be beneficial since that they can stabilize the tin compounds by coordination [48]. Finally, reagents such as $(n\text{-}Bu)_4N^+Ph_2P(O)O^-$ can act as a "tributyltin scavenger" to improve cross-coupling efficiency, as reported by Liebeskind and coworkers [49].

Another important category of additive is CuIor other Cu(I) salts, which could enhance coupling of Stille reaction, referred as the *copper effect*. Liebeskind and coworkers studied the effect of addition of CuI on the kinetics of Pd-catalyzed coupling between iodobenzene and vinyltributyltin in dioxane [50]. They observed a >100-fold rate increase when a strong ligand, such as PPh_3, was used, but little effect when a soft ligand, such as $AsPh_3$, was used. They concluded that CuI is a scavenger for the free ligand, especially for strong ligands such as PPh_3, which is known to inhibit the transmetallation. In addition, they proposed that in very polar solvents such as NMP and in the absence of strong ligand, a Sn/Cu transmetallation takes place to yield an organocopper species, which more easily transmetallates to the Pd(II) complex. They also observed that a stoichiometric ratio of $Pd:L:Cu = 1:4:2$ (L = ligands) gave the best result with both enhanced reaction rate and yield. Further increase of CuI did not increase the rates significantly, but did decrease the yield, because too much CuI removes ligand from the active catalytic species and thus reduces the catalyst stability. Many other Cu(I) salts (CuX, X = Cl, Br, CN, thiophene-2-carboxylate (TC)) have been reported to have similar effect [51–53].

1.3.4 Temperature

Though heating is applied in common Stille reactions, the reaction temperature plays a less important role than the other parameters discussed above, which have largely determined the catalytic cycle already. While temperature generally does not change the reaction pathway, it affects the Stille coupling in many aspects. For example, increasing temperature may improve the reaction rate and perhaps the solubility of relative compounds, especially in the case of Stille polycondensations. On the contrary, possible side reactions and decomposition, if the reagents are not stable against heat, may also take place at higher temperatures. However, high temperature of over 100 °C is usually employed for polymerization. High temperature increases the solubility of the resulting polymers in the reaction mixture so as to keep polymers in solution as the chain grows as long as possible; therefore, high molecular weight and narrow dispersity can be achieved.

From a practical perspective, inexpensive reagents (such as the previously mentioned aryl chlorides), lower reaction temperature, and shorter reaction time are desirable to save resources. Fu and coworkers [37, 47] further developed a room-temperature Stille coupling for aryl bromides. Meanwhile, new ways of heating have been studied to increase heating efficiency. Microwave irradiation has been used in the Stille reaction to reduce the reaction time from hours or days, as in conventional oil bath reactions, to minutes, with only a limited reduction in yield (Scheme 1.14) [54]. This technique enables a more timely way of reaction condition optimization. In this case, energy is directly transferred to the reactants and the temperature of the whole volume rises simultaneously (bulk heating); while in an oil bath, the reaction mixture in contact with the vessel wall is heated first [55]. Microwave-assisted heating has been found to be useful in Stille polycondensation to produce polymers of better quality. For example, Bazan and coworkers reported the synthesis of a low band gap polymer for solar cell applications from dibromobenzothiadiazole and distannylated dithienosilole (DTS). The use of microwave irradiation resulted in improved molecular weight of $M_n = 14-22$ kDa with yields as high as 80%, as well as promising power conversion efficiencies as high as 5.9% [56].
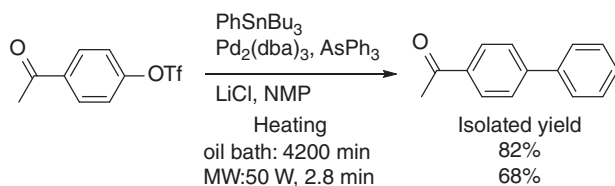
Scheme 1.14 Microwave conditions to shorten reaction time [54].

1.4 Examples of Functional Materials Synthesized by Stille Polycondensation

Due to the tolerance of the Stille reaction toward many different functional groups, the Stille polycondensation is ideal for the synthesis of functional polymers. The first functional polymer synthesized with Stille polycondensation is poly(phenylene-thiophene) (PPT) which was shown to exhibit liquid crystal (LC) properties and nonlinear optical (NLO) properties (Scheme 1.4) [17]. By changing the length of the side chains, physical properties of the polymers, such as phase transition temperatures, solubility, and fusibility, may be fine-tuned. The broad scope of this polycondensation reaction is well demonstrated by Yu *et al.*, who in 1995 synthesized polymers containing metalloporphyrin and carbazole moieties (Scheme 1.5) [18]. Since then, this synthetic approach has emerged as a standard approach toward numerous polyaromatic conjugated polymers exhibiting a range of appealing physical properties. The following section documents typical examples of these polymers and a brief introduction of their applications.

1.4.1 Nonlinear Optical (NLO) polymers

1.4.1.1 Background

Nonlinear optics describes the behavior of light in nonlinear media. The dielectric polarization P of the media responds nonlinearly to the electromagnetic field E of an intense light, such as from a laser, which in return affects the behavior of light, including phase, frequency, and amplitude. The relationship of P and E follows the equation

$$P = P_0 + \chi_{ij}^{(1)} E_{ij} + \chi_{ijk}^{(2)} E_j E_k + \chi_{ijkl}^{(3)} E_j E_k E_l + \cdots$$

where P_0 is the static dipole moment and $\chi^{(n)}$ is the nth order susceptibility. The term $\chi^{(1)}$ describes normal linear behavior (refraction and absorption) and the rest describes nonlinear behavior. The $\chi^{(n)}$ values are nonzero for all media when n is an odd number. When n is an even number, $\chi^{(n)}$ is nonzero only when the media is noncentrosymmetric. NLO materials, particularly second-order NLO, can be very useful in information technology, where light can be used as an information carrier to process, transmit, and store data at extremely high speed. In general, $\chi^{(n)}$ values are small when $n > 3$ and thus only the $\chi^{(2)}$ and $\chi^{(3)}$ parameters are of significant value for possible real-world applications. For materials to be useful in NLO applications, they should display low optical losses from either absorption or scattering, fast response times, easy processability, as well as high chemical and optical stability [7]. Polymers with large second-order optical nonlinearity are usually those containing oriented NLO chromophores with large dipole moments and conjugated polymers have emerged as an important class of third-order NLO materials.

1.4.1.2 Examples of NLO Polymers Synthesized by Stille Polycondensation

Second-order NLO materials are very promising for photonic applications, because they exhibit a linear electro-optic effect in which the refractive index of the material can be controlled by an applied external E [57]. A polymer containing NLO chromophores will become noncentrosymmetric when the chromophores are oriented by applying high external electric field via field–dipole interaction at an elevated temperature, usually past their glass transition temperature, T_g [57, 58]. Cooling will freeze this orientation, resulting in a material with second-order nonlinearity. In polar polymers, this orientation order should be kept over time even at increased temperature in order to maintain second-order nonlinearity.

In order to synthesize these polymers, NLO chromophores are usually either grafted as side chains or imparted into the polymer backbone (**8**, Scheme 1.15) [59–61]. To achieve large second-order optical nonlinearity exhibiting high thermal stability in dipole orientation, chromophores with large dipole moments are incorporated to polyimide chains. Unfortunately, these chromophores are usually sensitive to traditional synthetic approaches of polyimides. In order to solve this problem, Yu and coworkers utilized the mild reaction conditions of Stille polycondensation to synthesize functional polyimides. A polyimide derivative (**9**) with an amino chromophore side chain was synthesized (Scheme 1.16) [62]. In the same report, another polymer (**10**) with a similar chromophore but different polymer backbone was also prepared. Polymer **9** showed higher T_g than **10** (170 and 125 °C, respectively), possibly due to the higher

molecular weight. Interestingly, while the loading density of chromophore decreased from 65.04% in **10** to 50.85% in **9**, the r_{33} value increased from 9 to 35 pm V^{-1}, indicating a higher orientational stability of the chromophores in **9**. The authors proposed that higher loading will decrease the average distance between chromophores, resulting in increased dipolar repulsion between chromophores, which reduces the electro-optic effect.
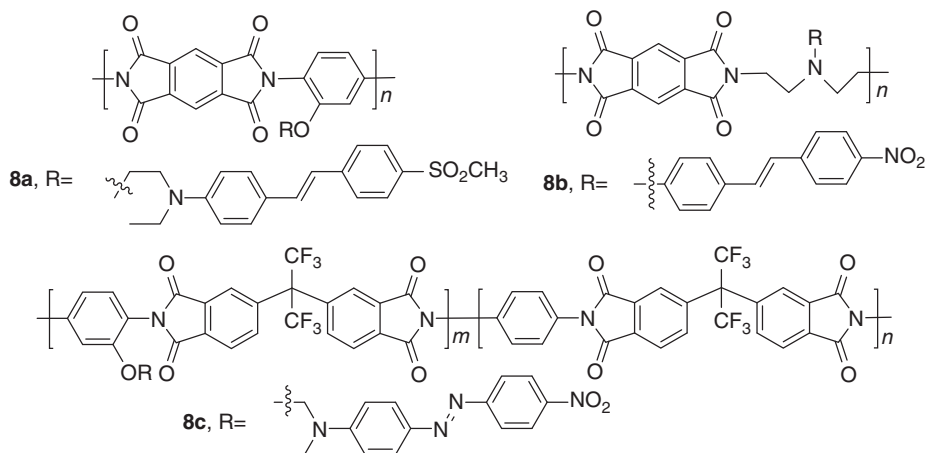

Scheme 1.15 The structure of some polyimide polymers for second-order NLO [59–61].

Third-order nonlinear optic effect can be observed in centrosymmetric media, caused by displacement of electron distribution. This effect is large when the density of polarizable electrons is high, such as in the case of conjugated polymers. Numerous conjugated polymers, such as polyphenylenevinylene (PPV) and polythiophene derivatives, were studied and shown to exhibit interesting third-order NLO properties. For example, Yu and coworkers synthesized a series of PPT polymers by Stille polycondensation with Pd(PPh$_3$)$_2$Cl$_2$ catalyst in THF solvent (Scheme 1.4). The polymer with $-$OC$_{16}$H$_{33}$ side chains showed a third-order nonlinear susceptibility $\chi^{(3)}$ of 1.77×10^{-13} esu in CHCl$_3$ solution [16]. Naso and coworkers synthesized tetrafluoro- and dialkoxy-substituted PPV polymers with high percentage of fluorinated units (>60%) via Stille polycondensation (**11**, Scheme 1.17) [63]. Fluorinated PPV gave more than 10 times higher third-order susceptibility, $\chi^{(3)}$ ($6 \pm 2 \times 10^{-10}$ esu), than that of the nonfluorinated one. Schrof and coworkers prepared a series of conjugated polymers, including random copolymers, based on a polythiophene backbone through Stille polycondensation (**12**, Scheme 1.18) [64]. These polymers showed red and near-infrared (IR) absorption and high third-order nonlinear behavior with $\chi^{(3)}$ value as high as 10^{-8} esu.

Photorefractive (PR) polymers are also an important class of NLO materials. The PR effect describes the change in the refractive index of a certain material in response to light of varying intensity, under the illumination of low-power lasers. A PR material can be used to record and store optically encoded information such as holograms [57]. A PR polymer normally needs two functions: photoconductivity and electro-optic effect. It consists of a photocharge generator, a charge transporter, a charge trapping center, and an NLO chromophore. For example, Yu and coworkers [65] made PPT derivative
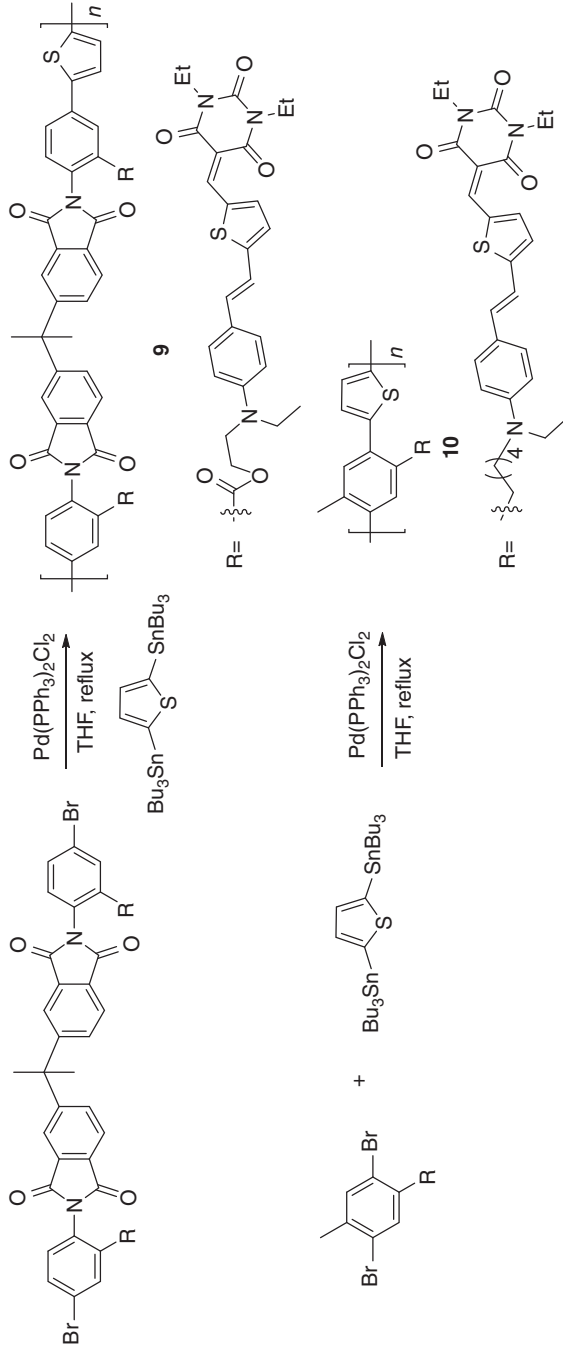
Scheme 1.16 Synthesis of polymers with NLO chromophores on side chains [62].
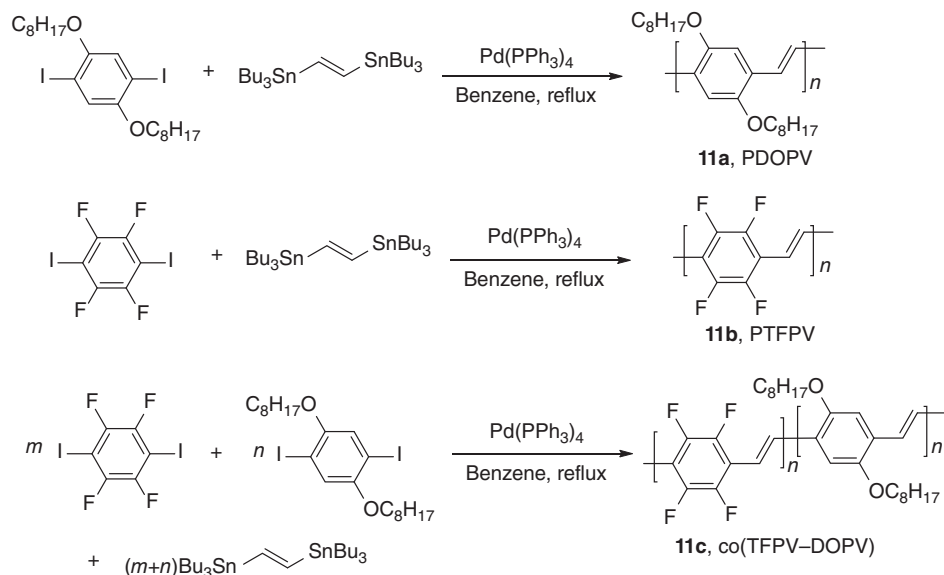
**Scheme 1.17** Synthesis of fluoro- and alkoxy-substituted PPVs for third-order NLO [63].
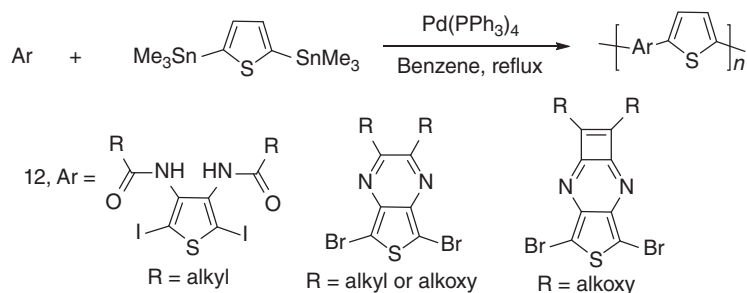
Scheme 1.18 Synthesis of polythiophene derivatives for third-order NLO [64].

polymers **13** via Stille polycondensation (Scheme 1.19). These polymers were PR; a side chain contained an electron-rich amino unit and an electron-withdrawing tricyanodihydrofuran group, creating a strong dipole and thus serving as a second-order NLO chromophore; while the conjugated backbone absorbs visible light with a maximum at about 590 nm and acted as a charge generator and transporter. The best PR results were obtained for **13a,** with a net optical gain coefficient of $158\,cm^{-1}$ at a field of $50\,V\,\mu m^{-1}$ and a diffraction efficiency of 68% at a field of $46\,V\,\mu m^{-1}$. The synthesis of these multifunctional polymers is difficult with other synthetic approaches due to the sensitivity of NLO chromophores to both basic and acidic conditions, and demonstrated the broad utility of the Stille polycondensation.

1.4.2 Organic Photovoltaic Polymers

1.4.2.1 Background
The triumph of the Stille polycondensation is its broad application in the synthesis of donor–acceptor (D–A) semiconducting polymers for OPV solar cell applications.
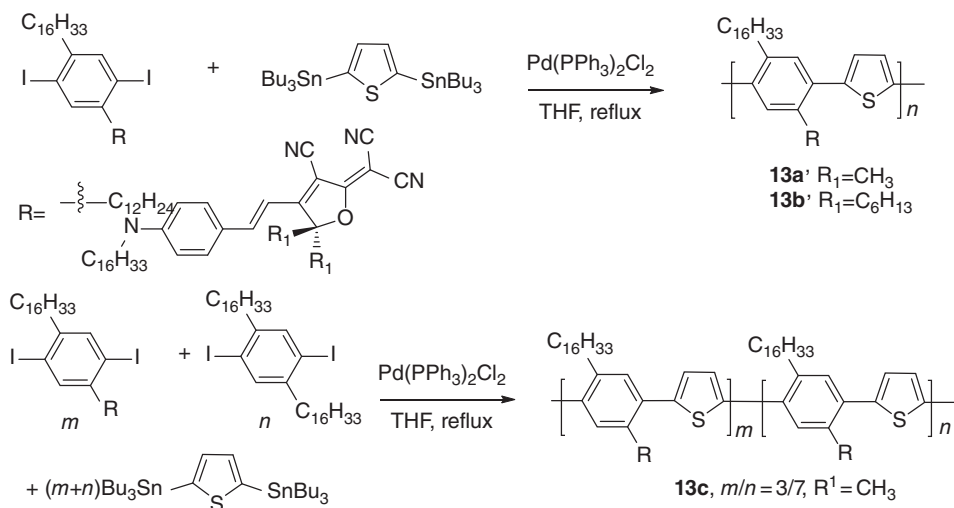
Scheme 1.19 Synthesis of PPTs with tricyanodihydrofuran subunit for PR material [65]

Polymer solar cells (PSCs) for the conversion of solar energy into electricity have been studied extensively in the past decades for their potential in fabricating lightweight and flexible devices, as well as their high-throughput production process and potential low cost [8]. Currently, the bulk heterojunction (BHJ) architecture is the most widely studied design for PSCs, in which donor and acceptor materials are mixed together to form a bicontinuous interpenetrating network between two electrodes. Typically, the donor material is a conjugated polymer, and the acceptor material is a fullerene derivative, such as [6,6]-phenyl C_{61} butyric acid methyl ester (PCBM, which may also refer to the close analog [6,6]-phenyl C_{71} butyric acid methyl ester). Another system, which has been gaining popularity recently, is the all polymer cell, where the fullerene is replaced by another conjugated polymer as acceptor material. The Stille polycondensation has made an irreplaceable contribution to the development of both donor and acceptor polymers.

1.4.2.2 Examples of Donor Polymers

Donor polymers play a key role in BHJ solar cells, because they are the main component for the absorption of light and the generation of electrical current. The common rules for donor polymers include: low band gap to absorb as much solar energy as possible, correct energy level match with the acceptor material, good solubility in common solvents, and miscibility with the acceptor material to form the desired nanoscale morphology, all of which require careful selection of backbone structure, side chains, and substituent groups.

The first polymers for BHJ PSCs were PPV derivatives [66, 67], but their application was limited by the large band gaps (>2 eV) and low photocurrent. Later research interest shifted to polythiophenes, especially poly(3-hexylthiophene-2,5-diyl) (P3HT) [68], which is still a heavily studied system to this day [69]. Regioregular P3HT is normally synthesized by the McCullough method [70]. The Stille polycondensation is also applicable to the synthesis of some polyalkylthiophenes. For example, Yang and coworkers
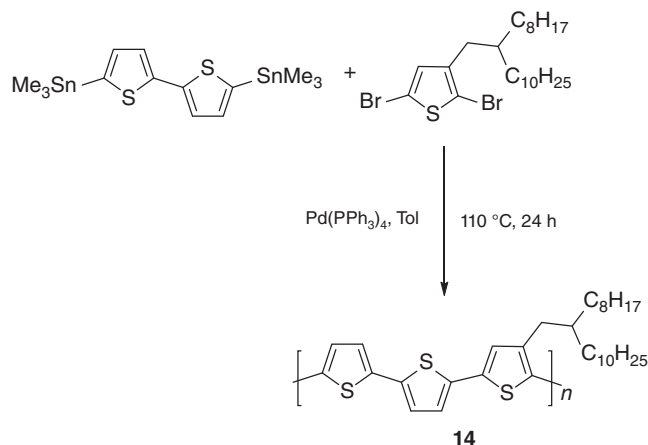
Scheme 1.20 Synthesis of a polyalkylthiophene polymer [71].

(**14**, Scheme 1.20) [71] synthesized a regioregular polythiophene, bearing fewer alkyl chains than typical polyalkylthiophenes, using $Pd(PPh_3)_4$ as the catalyst and toluene as the solvent at 110 °C. This system resulted in a polymer with $M_w = 18.9$ kDa and dispersity (Đ) $= 1.8$. A maximum power conversion efficiency (PCE) of 3.4% was achieved in the polymer/PCBM devices.

The most recent breakthrough in the design of solar cell polymers has been the introduction of D−A alternating copolymers [42, 72−74]. Unlike homopolymer P3HT, where a single moiety is used as the repeating unit, these low band gap polymers incorporate a backbone, which alternates between one electron-rich moiety (donor) and one electron-deficient moiety (acceptor). One unique feature of these polymers is that their HOMO and LUMO energy levels are largely determined by the HOMO energy level of the donor and the LUMO energy level of the acceptor, respectively [75]. Therefore, the energy levels of polymers can be tuned by modifying the donor and acceptor units separately by introducing different functional groups [7, 76]. Due to its tolerance of a wide variety of functional groups, the Stille polycondensation is highly competitive for the synthesis of these polymers. Some design principles for the construction of D−A copolymers are that the building moieties should have proper electron-donating or -accepting abilities, available sites for side chain and functional group modifications, and are favorable for conjugated polymer propagation. Through these rules, and the use of the Stille polycondensation, many high-performance polymers have been developed by combining various donor and acceptor moieties.

The benzo[1,2-*b*:4,5-*b*′]dithiophene (BDT) unit is an important electron-rich building block for high-performance solar cell polymers. The PTB series of polymers incorporating BDT and thieno[3,2-*b*]thiophene (TT), developed by Yu and coworkers, showed excellent solar cell performance [74, 77, 78]. They were prepared by Stille polycondensation, with $Pd(PPh_3)_4$ catalyst, toluene/DMF mixed solvent at 120 °C (Scheme 1.21). High molecular weight can be obtained for polymers of this series due to their excellent solubility, which allows them to stay in solution in the reaction mixture until the growing polymer chains are very large. These polymers were widely investigated for OPV cells [78]. Developed in 2010, PTB7, when combined with
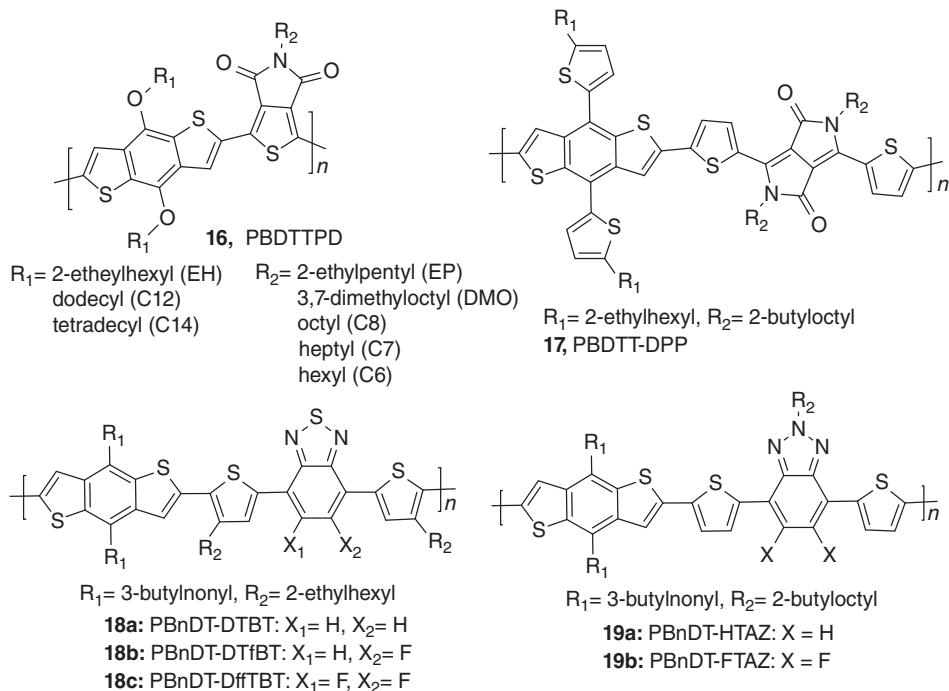
Scheme 1.21 Synthesis of PTB polymers.
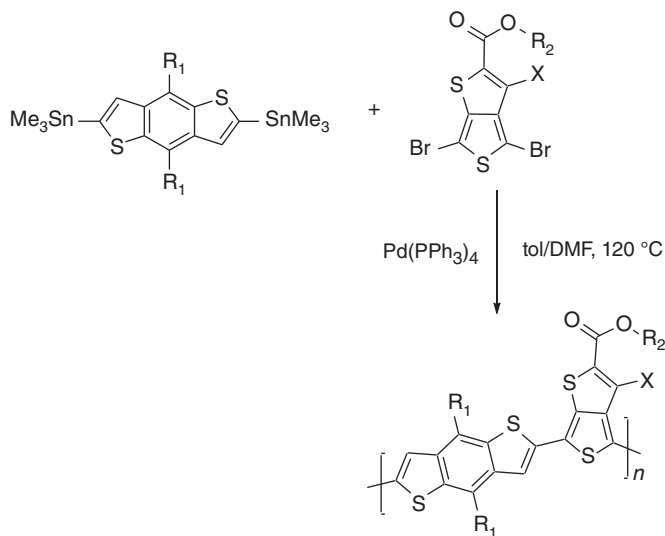
15a: PTB1: X = H, R$_1$= *n*-octyloxy,   R$_2$= *n*-dodecyl
15b: PTB2: X = H, R$_1$= *n*-octyloxy,   R$_2$= 2-ethylhexyl
15c: PTB3: X = H, R$_1$= *n*-octyl,   R$_2$= 2-ethylhexyl
15d: PTB4: X = F, R$_1$= 2-ethylhexyloxy, R$_2$= *n*-octyl
15e: PTB5: X = H, R$_1$= 2-ethylhexyloxy, R$_2$= *n*-octyl
15f: PTB6: X = H, R$_1$= *n*-octyloxy,   R$_2$= 2-butyloctyl
15g: PTB7: X = F, R$_1$= 2-ethylhexyloxy, R$_2$= 2-ethylhexyl
15h: PTB7-Th: X = F, R$_1$= 5-(2-ethylhexyl)thienyl, R$_2$= 2-ethylhexyl

PC$_{71}$BM, achieved a PCE of 7.4%, which was a record at that time [74]. Further device engineering pushed the PCE of a PTB7 single-junction device to 9.2% via an inverted device structure, which switches the nature of the transparent and metal electrodes [79]. Yu and coworkers also synthesized fluorinated derivatives of PTB polymers to study the effect of fluorine substitution on the performance of PTB polymers [80]. It was found that fluorination on the TT unit enhances the polarization of polymers, facilitating charge separation. Yu and coworkers also synthesized PTB polymers with enhanced 2-D character of the π-bonding system by grafting aromatic side chains to the BDT unit to improve the coplanarity of the polymer backbone. This arrangement favors π-stacking and charge transport properties, resulting in several patented polymers with alternating Fluorinated TT and BDT-Th units [81]. The same strategy was used by other research groups [82]. Using inverted device architecture, Cao and coworkers were able to reach a PCE of 9.94% from PTB7-Th/PC71BM blend [83]. In addition to PTB series, there are many other high-performance donor polymers incorporating BDT with other electron-deficient monomers (Scheme 1.22) [73, 84–89].
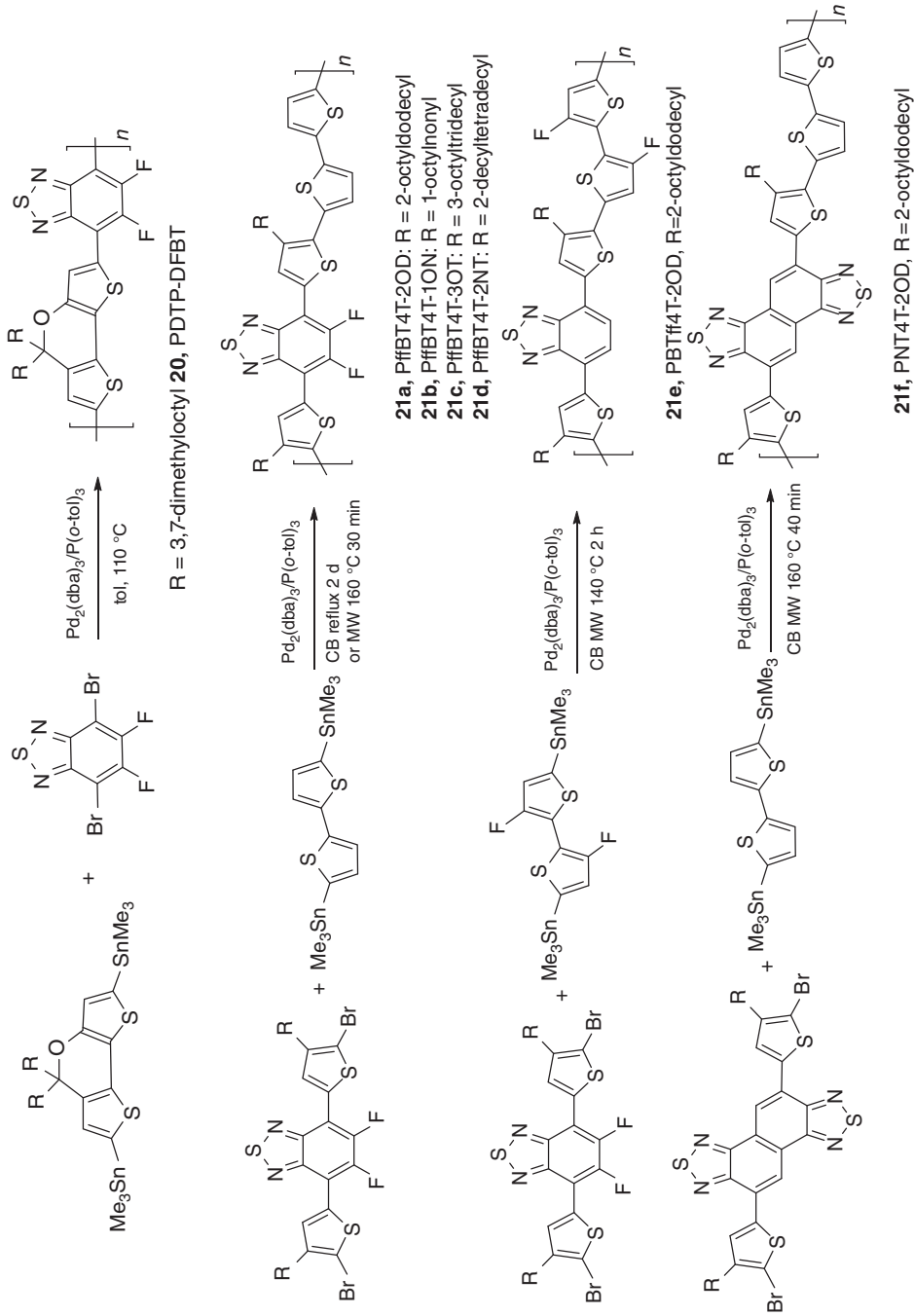
Benzothiadiazole (BT) is also an attractive electron-deficient building block for the synthesis of solar cell polymers via Stille polycondensation. A useful derivative of BT is dithienyl benzothiadiazole (DTBT), which is generated by adding two flanking thienyl groups to the BT unit. This enhances the coplanar structure of resulting polymers, as well as provides more sites for further functionalization. These two monomers and
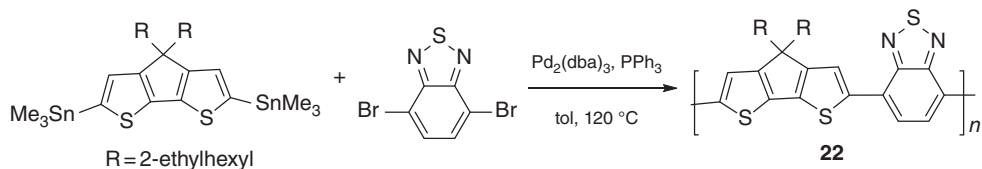
R_1 = 2-etheylhexyl (EH)
  dodecyl (C12)
  tetradecyl (C14)

R_2 = 2-ethylpentyl (EP)
  3,7-dimethyloctyl (DMO)
  octyl (C8)
  heptyl (C7)
  hexyl (C6)

16, PBDTTPD

R_1 = 2-ethylhexyl, R_2 = 2-butyloctyl
17, PBDTT-DPP

R_1 = 3-butylnonyl, R_2 = 2-ethylhexyl
18a: PBnDT-DTBT: X_1 = H, X_2 = H
18b: PBnDT-DTfBT: X_1 = H, X_2 = F
18c: PBnDT-DffTBT: X_1 = F, X_2 = F

R_1 = 3-butylnonyl, R_2 = 2-butyloctyl
19a: PBnDT-HTAZ: X = H
19b: PBnDT-FTAZ: X = F

Scheme 1.22 The structures of PBDTTPD [73, 84–86], PBnDT-DTBT [87], PBnDT-FTAZ [88], and PBDTT-DPP [89].

their derivatives are widely used to generate high-performance polymers. For example, Yang and coworkers [90] synthesized a polymer with difluoro-substituted benzothiadiazole (DFBT) using Stille polycondensation (**20**, Scheme 1.23). The resulting polymer PDTP–DFBT obtained a PCE of 7.9% due to the polymer having a low band gap, which allowed broad absorption over longer wavelengths than typical donor polymers. Interestingly, the authors then made tandem solar cells with PDTP–DFBT and P3HT, the latter of which has strong absorption at shorter wavelengths, leading to a PCE of 10.6% due to the complementary nature of the two polymers allowing strong absorption throughout the whole visible and near-IR region. More recently, Yan and coworkers have made a series of polymers with DTBT and studied the effect of the side chain on the solar cell performance of the resulting polymers (**21**, Scheme 1.23) [42]. It was indicated that right size and position of branched side chains would give polymers high crystallinity, pure domain, and proper domain sizes, resulting in high performance, the best being PffBT4T-2OD, which gave PCE as high as 10.8% when combined with a custom fullerene acceptor. Interestingly for the synthetic chemist, two different Stille polycondensation methods were used, employing both conventional and microwave heating. It was found that molecular weight was largely determined by the nature of the substrate rather than the nature of the heating, though microwave irradiation significantly shortened the reaction time compared to conventional heating.

4H-cyclopenta[2,1-*b*:3,4-*b*′]dithiophene (CPDT) is a widely employed electron-rich monomer for solar cell polymers. The planar structure can reduce the band gap of the polymer and improve charge carrier mobility. In addition, the tetrahedral carbon center provides sites for side chains and improves the solubility, as well as affects the packing

R = 3,7-dimethyloctyl **20**, PDTP-DFBT

21a, PffBT4T-2OD: R = 2-octyldodecyl
21b, PffBT4T-1ON: R = 1-octylnonyl
21c, PffBT4T-3OT: R = 3-octyltridecyl
21d, PffBT4T-2NT: R = 2-decyltetradecyl

21e, PBTff4T-2OD, R=2-octyldodecyl

21f, PNT4T-2OD, R=2-octyldodecyl

Scheme 1.23 Synthesis of PDTP-DFBT [90], PffBT4T, PBTff4T, and PNT4T [42].

**Scheme 1.24** Synthesis of CPDT-BT polymer [91, 92].
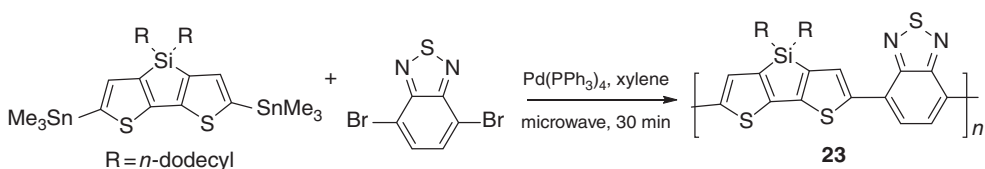
Scheme 1.25 Synthesis of Si-bridged CPDT-BT polymer [56].

property of polymer in solid state. Close derivatives may be formed by the replacement of the carbon center with heteroatoms such as Si or Ge. Several groups have reported the copolymerization of CPDT with different alkyl chains and BT using Stille conditions with $Pd_2(dba)_3/PPh_3$ in toluene at 120 °C (**22**, Scheme 1.24) [91, 92]. These polymers showed sizable molecular weight and were relatively narrow dispersities, with PCEs around 3.5% obtained from polymer/PCBM devices and can be improved to 5−8%.

Changing the bridging carbon to silicon, polymer **23** was synthesized by Bazan and coworkers (Scheme 1.25) using Stille conditions but two different methods of heating [56]. The conventional heating generated polymers with $M_n = 7−10$ kDa, while those produced with microwave irradiation reached 44 kDa. Typical of the field, the polymer with higher molecular weight showed a much higher current density (J_{sc}) in a solar cell device, which is known to correlate with increased light absorption.

Ge-substituted CPDT has also been reported. Reynolds and coworkers employed both DTS and dithienogermole (DTG) as the donor unit and thienopyrroledione (TPD) as the acceptor unit to produce low band gap polymers (Scheme 1.26) under Stille conditions with $Pd_2(dba)_3/P(o\text{-tol})_3$ in toluene at 115 °C [93]. Relatively high molecular weight ($M_n = 31−48$ kDa) and low polydispersity (around 1.7) were obtained. The bond length of C−Ge (3.27 Å) is longer than that of C−Si (3.11 Å), as determined from the distance between the substituent methyl group and the nearest carbon atom in the thiophene unit. The PCE for PDTG−TPD (**24b**) (7.3%) is higher than that of PDTS−TPD (**24a**) (6.6%) due to better J_{sc} and FF. However, in another report by Tao and coworkers, the PCE of PDTS−TPD reached 7.3% [94]. Later, the PCE of PDTG−TPD was further improved to 8.5% after careful device engineering by the Reynolds group [95].

Isoindigo (IID) is a very planar molecule and can be employed to synthesize solar cell polymers. For example, Andersson and coworkers made a polymer with IID and terthiophene oligomer P3TI (**25**, Scheme 1.27) [96]. It showed low band gap of 1.5 eV and the terthiophene unit facilitated better stacking of polymer chains. As a result, a PCE of 6.3% was obtained. Bao and coworkers [97] also prepared an IID-based random copolymer with low molecular weight polystyrene (PS) side chains using microwave-assisted Stille polycondensation (**26**, Scheme 1.27). The solubility was enhanced and the best
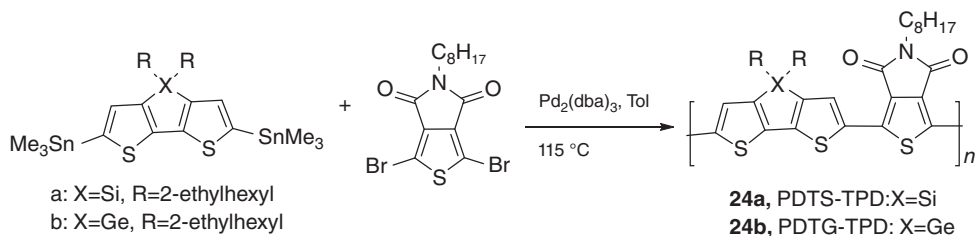
Scheme 1.26 Synthesis of Si- and Ge-bridged CPDT-TPD polymers [93–95].

PCE can reach 7.0% after preparative Size Exclusion Chromatography purification of the polymers.
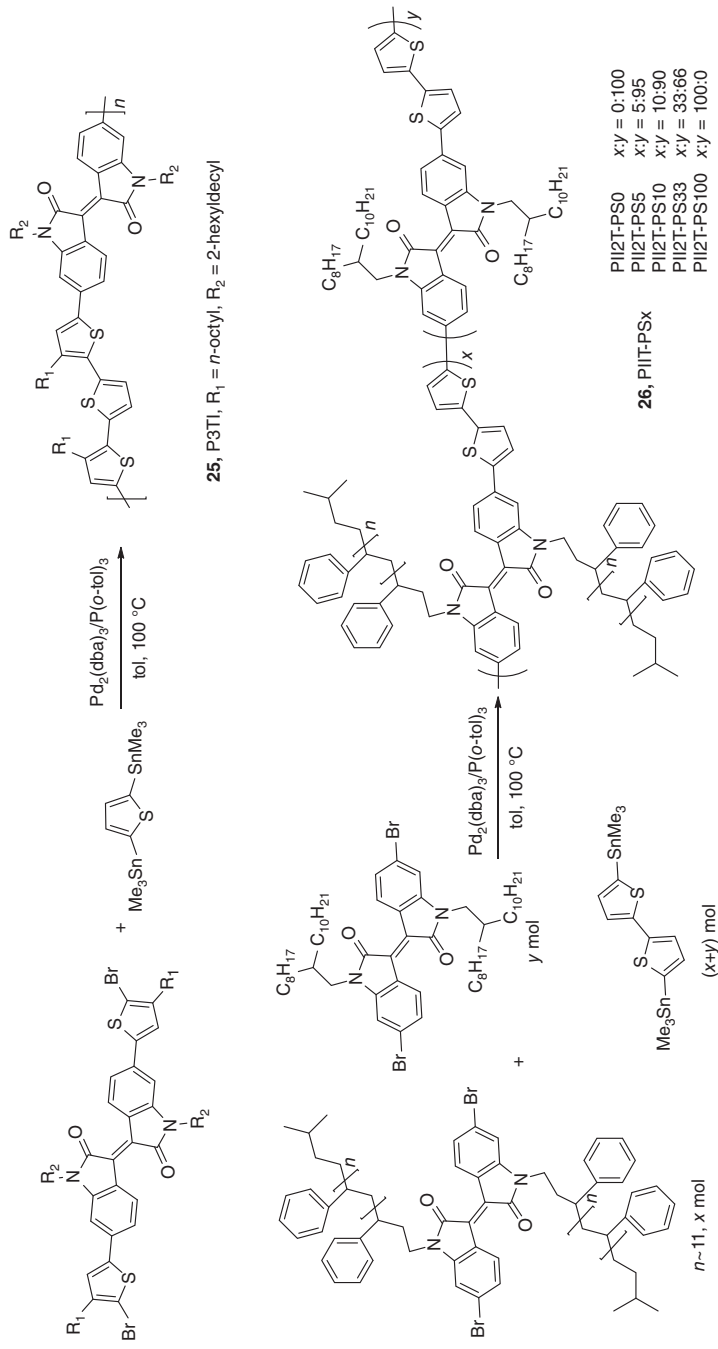
In recent years, lactam-bridged heterocycles have been developed as promising building blocks for high-performance donor polymers for solar cells. Ding and coworkers have made a series of donor polymers with different types of lactam monomers using Stille polycondensation (Scheme 1.28) [98–102]. With pentacyclic lactam units, the polymers **27a–27d** showed maximum PCE values from 3.5% to 5.3% in the polymer/$PC_{71}BM$ solar cells [98]. By changing the Ar units to selenophene or thiophene, better performance may be achieved. The copolymer with selenophene, **27e** showed high molecular weight ($M_n = 34.9$ kDa) and very high dispersity (Đ = 3.51), as well as a particularly low-lying HOMO level of −5.41 eV and a high organic field effect transistor (OFET) hole mobility at 0.26 cm^2 (V s)$^{-1}$. The PCE of **27f**/$PC_{71}BM$ solar cells could reach 6.04% [99]. **27f**/$PC_{71}BM$ cells showed higher PCE of 9.20% in inverted device structures [100]. They have also made polymers with hexacyclic lactam monomers (**28**). Compared to thiophene copolymers, selenophene analogs, **28c** and **28d** exhibited better solar cell properties. A maximum PCE of 8.2% was achieved in inverted **28d**/$PC_{71}BM$ solar cells [101]. Incorporating a new lactam monomer and thiophene unit, **29** has been synthesized resulting in **29**/$PC_{71}BM$ solar cells characterized by high voltage and appreciable PCE values in both conventional and inverted device structures (7.9% and 9.1%, respectively) [102].

While most of the Stille condition discussed above used $Pd(PPh_3)_4$ or $Pd_2(dba)_3$ as the catalyst, some polymers were synthesized using different catalysts. For example, Kreds and coworkers used $Pd(PPh_3)_2Cl_2$ in THF solvent to synthesize a series of low band gap polymers (**30**, Scheme 1.29) [103].
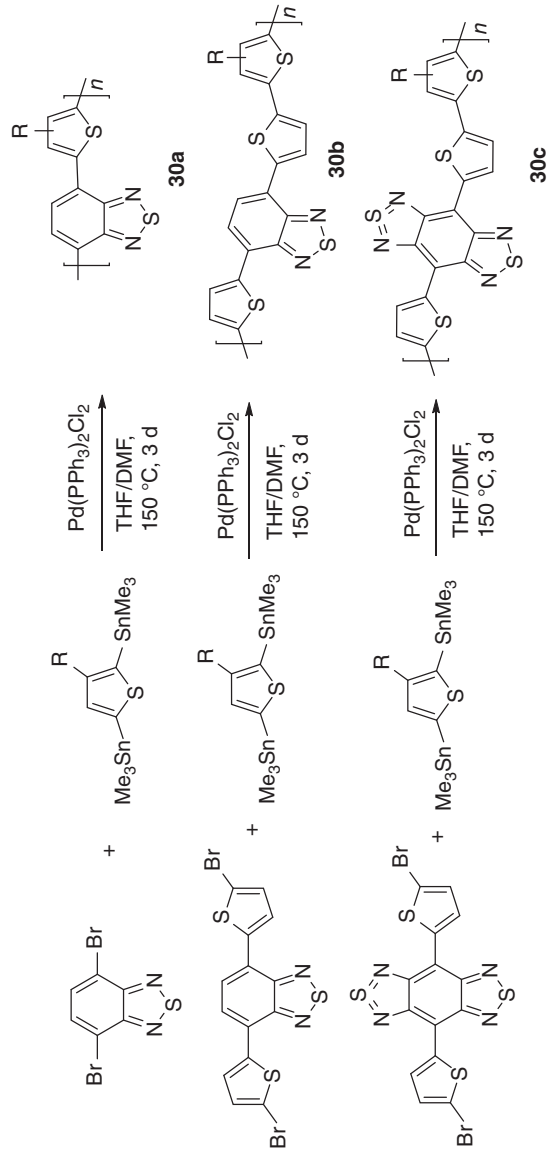
1.4.2.3 Examples of Acceptor Materials

Though the acceptor materials for PSCs are dominated by fullerene and its derivatives, polymer acceptor materials are developing rapidly. Their advantages include potentially lower cost, and easier modification of physical properties. To compete with fullerenes, acceptor polymers should have (i) well-matched energy levels with donor polymers, (ii) strong and broad absorption in the visible range, (iii) high electron mobility for efficient charge transport, and (iv) good solubility and miscibility with donor polymers to form a phase-separated BHJ structure. As with donor polymers, Stille polycondensation is a versatile method in preparing acceptor polymers.

Pei and coworkers synthesized an acceptor polymer **31b** from di-thiazole-benzothiadiazole (DTABT) and indacenodithiophene (IDT) for the use of all-PSCs using microwave-assisted Stille polycondensation (Scheme 1.30) [104]. Compared to

25, P3TI, R$_1$ = n-octyl, R$_2$ = 2-hexyldecyl

26, PIIT-PSx

PII2T-PS0	x:y = 0:100
PII2T-PS5	x:y = 5:95
PII2T-PS10	x:y = 10:90
PII2T-PS33	x:y = 33:66
PII2T-PS100	x:y = 100:0

Scheme 1.27 Synthesis of IID-based polymers [96, 97].

Scheme 1.28 Synthesis of lactam-based donor polymers [98–102].

Scheme 1.29 Conjugated polymers based on thiophene, benzothiadiazole, and benzobis(thiadiazole) [103].
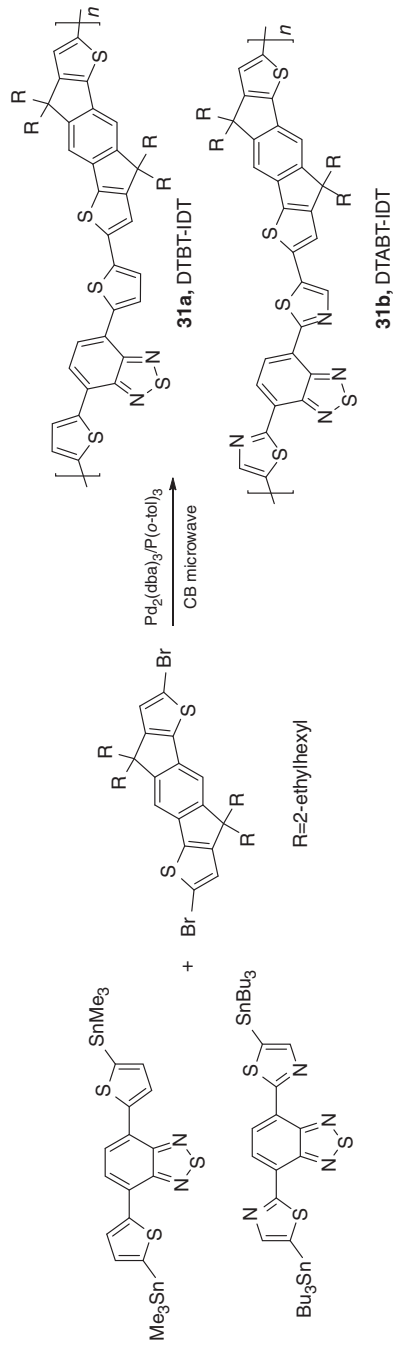
Scheme 1.30 Synthesis of DTBT-IDT and DTABT-IDT [104].

the **31a**, the LUMO energy levels of **31b** decreased from 3.21 to −3.45 eV, resulting in an enhancement of the electron mobility by two orders of magnitude, with a decrease in hole mobility. A PCE of 1.18% was obtained for the P3HT/**31b** device, higher than that of **31a** (0.85%), which was ascribed to the better miscibility of **31b** with P3HT.

Perylene-diimide (PDI) and its derivatives are promising acceptor materials and thus widely studied for their high electron mobility and strong intermolecular π-interaction. Marder and coworkers [105] synthesized a PDI-based polymer **32**, using conventional Stille conditions (Scheme 1.31). The final polymer exhibited relatively low molecular weight (15 kDa) low dispersity (1.5). It showed electron mobilities in the saturation regime as high as $1.3 \times 10^{-2} \, \mathrm{cm^2 \, V^{-1} \, s^{-1}}$. Zhan and coworkers reported an all-PSC incorporating PDI−DTT (**32a**) [106]. The addition of PDI−2DTT (**32b**), a small molecule fragment of the polymer **32a**, could enhance donor/acceptor mixing for more efficient charge transfer and thus improve the average PCE from 1.16% to 1.43%. Moreover, DIO improved the average PCE to 2.92% by facilitating the crystallization of donor polymer. Taking advantage of both of the two additives, PCE could reach 3.45%.

Naphthalene-diimide (NDI) is also a good building block for acceptor polymers. The most common polymer incorporating it, N2200 (also known as *P(NDI2OD-T2)*, (**33**)) was first synthesized by Facchetti and coworkers (Scheme 1.32), incorporating NDI and bithiophene units, and showed high electron mobility ($\sim 0.45 - 0.85 \, \mathrm{cm^2 \, V^{-1} \, s^{-1}}$) [107]. Kim and coworkers obtained over 4.5% PCE from PTB7-Th/N2200 devices with highly intermixed donor/acceptor domains, in which PTB7-Th and N2200 acquired a face-on π-stacking geometry [108]. DIO additive, which increased the crystallinity of donor/acceptor domains, enhanced electron mobility and J_{sc} in the devices. In another report, Ito and coworkers achieved a PCE of 5.73% for PTB7-Th/N2200 devices with a maximum external quantum efficiency (EQE) around 60% [109], due to the high charge generation and collection efficiency (both over 80%), which were comparable to those in devices with fullerene acceptor. More recently, Jenekhe and coworkers have developed a series of acceptor polymers with NDI and thiophene or selenophene units (Scheme 1.33), which showed competitive electron-accepting properties as with PCBM [110–112]. The series showed high molecular weight ($M_n = 23.9 - 79.0 \, \mathrm{kDa}$) and low dispersity (Đ = 1.2−2.3). Compounds **34a**, **34b**, and **34c** showed field effect electron mobilities of 2×10^{-4}, 2×10^{-3}, and $7 \times 10^{-3} \, \mathrm{cm^2 \, (V \, s)^{-1}}$, respectively [110]. When incorporated into all-PSCs with PTB7-Th/**34c** blend, the highest PCE reached 7.7% after optimization of device processing [112].

Jenekhe and coworkers also reported another type of acceptor polymers (and small molecules) based on tetraazaben-zodifluoranthene diimide (BFI) unit (Scheme 1.34) [113, 114]. The field effect electron mobilities could reach as high as $0.30 \, \mathrm{cm^2 \, (V \, s)^{-1}}$ for PBFI-T (**35a**) and a PCE of 2.6% was achieved in a PSEHTT/**35a** blend solar cell with **35a** being used as the acceptor polymer. Using a similar strategy, they have developed a series of BFI-based small molecules to be applied as electron acceptor material for polymer/PSCs recently [115, 116]. The maximum PCE reached 6.4% from PSEHTT/**35d** devices [116].
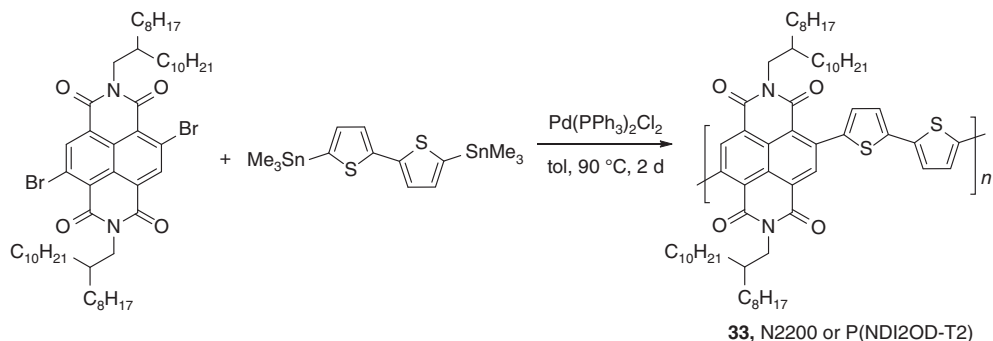
1.4.3 Organic Field Effect Transistor (OFET) Polymers
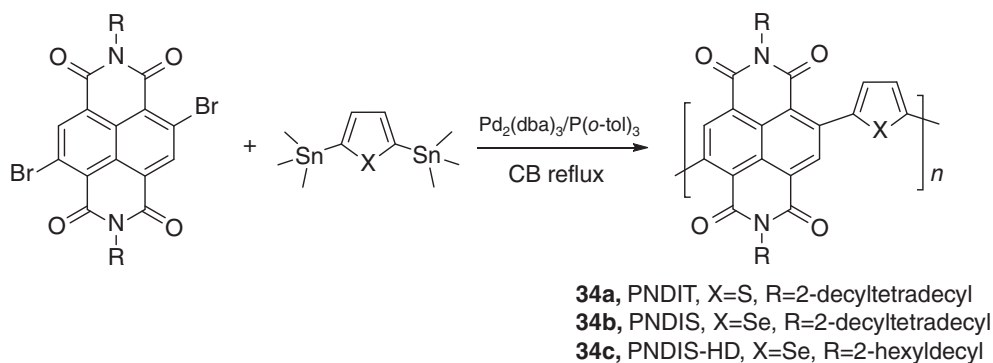
1.4.3.1 Background

FETs are another important application of organic semiconducting materials. Polymer-based FETs are lightweight, flexible, solution processable, and have low cost of
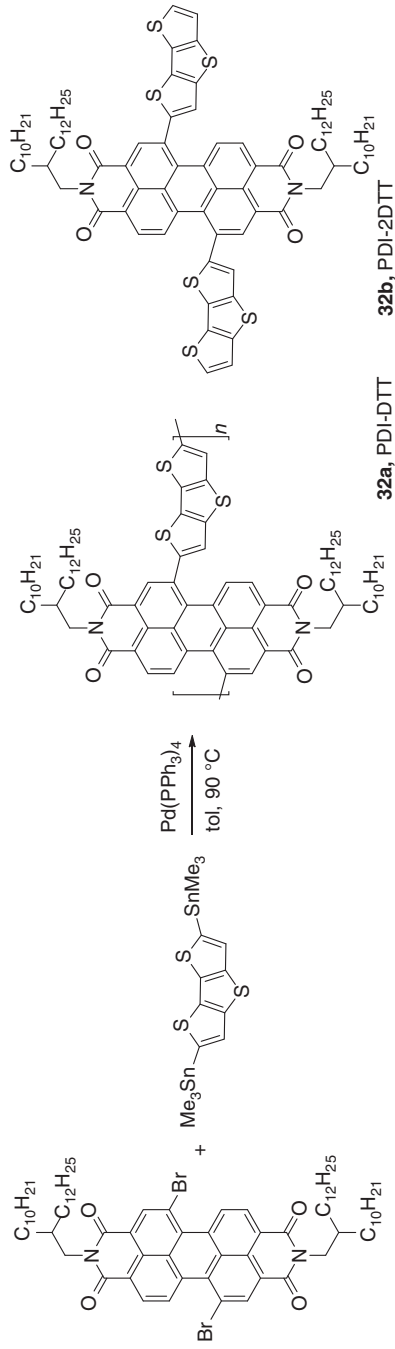
Scheme 1.31 The synthesis of PDI containing polymer and small molecule [105, 106].

Scheme 1.32 Synthesis of NDI-based polymer P(NDI2OD-T2) [107–109].

34a, PNDIT, X=S, R=2-decyltetradecyl
34b, PNDIS, X=Se, R=2-decyltetradecyl
34c, PNDIS-HD, X=Se, R=2-hexyldecyl

Scheme 1.33 Synthesis of PNDIT and PNDIS polymers [110–112].

fabrication, similar advantages to those described for OPV materials. A typical device for polymer FETs consists of a substrate, a gate electrode, a dielectric insulating layer, a source, and a drain electrode, between which a polymer semiconducting material is sandwiched. There is nearly zero current between the source and the drain electrode when the gate electrode is under zero bias. Application of nonzero bias to the gate electrode will generate an electric field at the polymer–insulator interface, which shifts the HOMO and LUMO energy levels of the semiconducting polymer. Therefore, a conducting channel between the source and drain electrodes is formed, where charge carriers can flow through the semiconducting polymers to electrodes to generate current. A key parameter for FETs is the charge carrier mobility, either electron mobility or hole mobility.

The development of polymers for FETs has been slow over the decades mainly because of the difficulties in synthesis and purification for obtaining high-quality semiconducting polymers. The charge carrier mobility is significantly lower than that of silicon FETs, and even lower than that of small-molecule OFETs. However, promising breakthroughs have been made in recent years with some polymers achieving charge carrier mobility values over $10 \, \mathrm{cm^2 \, V^{-1} \, s^{-1}}$ [117]. In addition to a high mobility value, for a semiconducting polymer to be used in OFETs, its energy levels (HOMO and LUMO) should match the work function of the electrodes. Finally, it should also have good chemical or thermal stability, as well as good crystalline properties, which are typically correlated
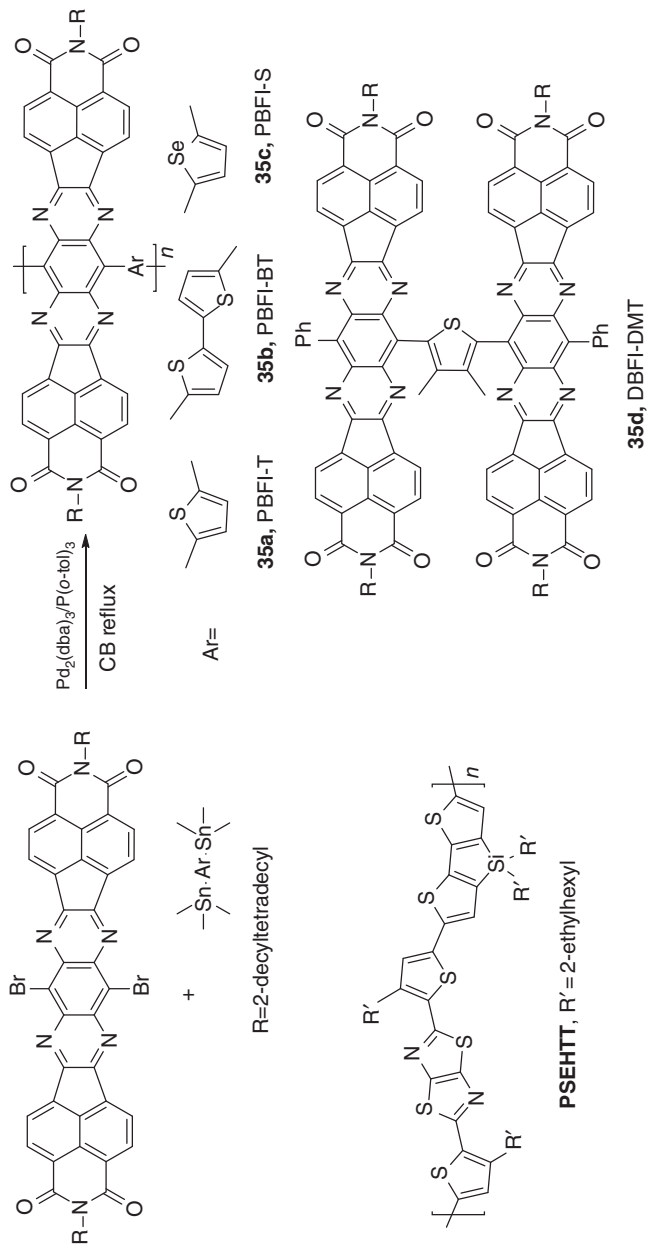
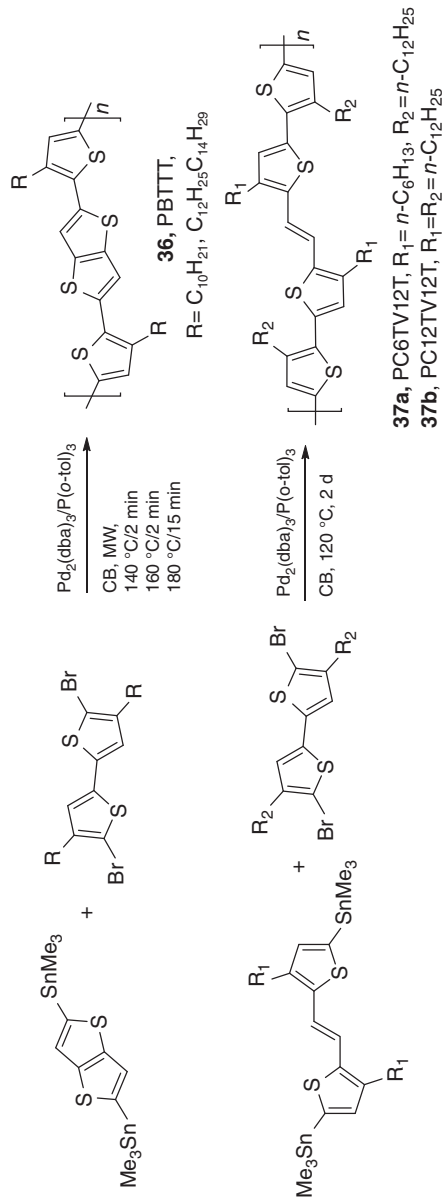**Scheme 1.34** Synthesis of BFI-based acceptor materials [113–116].

with high charge carrier mobility values. As with other types of conjugated polymers, Stille polycondensation is widely applied for the preparation of high-performance FET polymers.

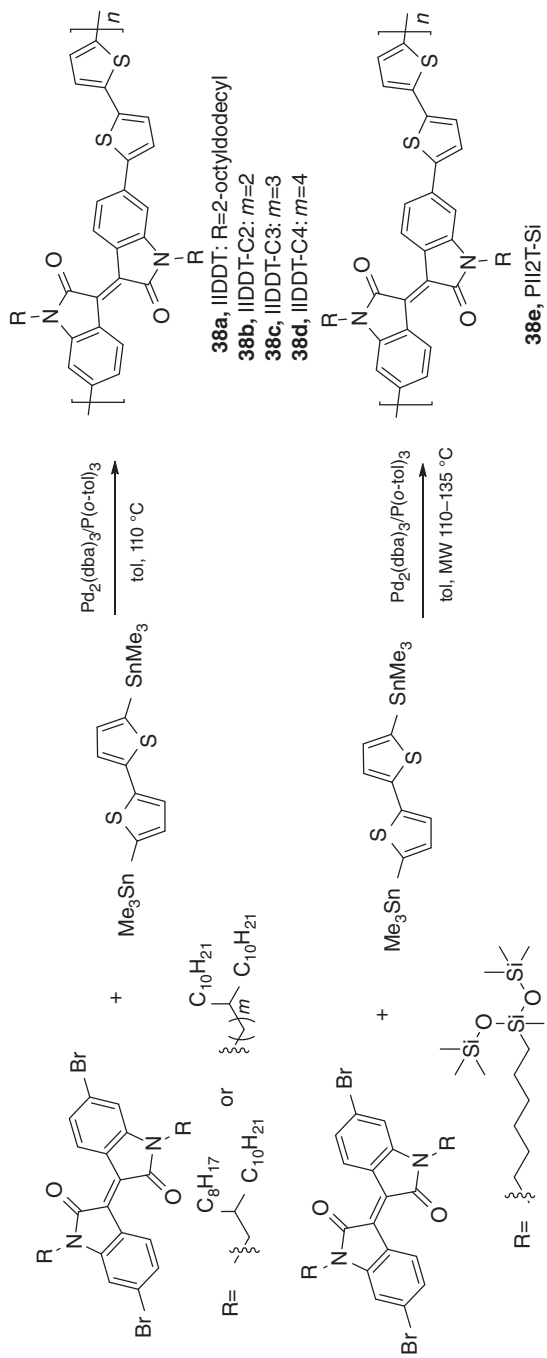### 1.4.3.2 Examples of FET Polymers Synthesized by Stille Polycondensation

Thiophene and its derivatives have been important building blocks for FET polymers since the 1990s, when P3HT was reported to exhibit a mobility of $0.1\,\mathrm{cm^2\,V^{-1}\,s^{-1}}$ [118]. Since then, much structural modification has been done on P3HT using Stille chemistry in order to improve the FET performance. For example, McCulloch and coworkers incorporated a fused thiophene unit into the polymer backbone to make the PBTTT polymer (**36**, Scheme 1.35) [119]. The polymers were synthesized via microwave-assisted Stille polycondensation with a stepwise temperature increase. PBTTT showed better stability than P3HT with 0.3 eV higher in ionization potential. The mobility was reported to be $0.2–0.7\,\mathrm{cm^2\,V^{-1}\,s^{-1}}$ under nitrogen with on/off ratio over 1×10^6. Kim and coworkers incorporated alkyl-substituted thienylenevinylene (TV) unit in the polythiophene backbone (**37**, Scheme 1.35) to improve the processability of polymers without decreasing their stability and performance [120]. A maximum carrier mobility of $1.05\,\mathrm{cm^2\,V^{-1}\,s^{-1}}$ was observed for **37b** with $I_{\mathrm{on}}/I_{\mathrm{off}}$ around 5×10^4 after annealing. The mobility was among the highest values for polythiophene semiconductors reported so far.

IID is a well-known building block for organic semiconducting materials. The IID core has poor solubility in common organic solvents due to the strong $\pi–\pi$ interaction and intermolecular hydrogen bonding between the hydrogens and the lactam nitrogens. However, the solubility can be improved by side chain modification on the nitrogen atoms to improve the processability of materials incorporating IID. Normally 6,6′-dibromo-IID is used as the starting monomer for polymerization, since 6,6′-linkage gives the polymers possible quinoidal resonance structure. For example, Pei and coworkers first reported an IID-based polymer **38a** with hole mobility over $1\,\mathrm{cm^2\,V^{-1}\,s^{-1}}$ in air-stable FET devices (Scheme 1.36) [121, 122]. Then, they studied the effect of the side chain branching position on the $\pi–\pi$ stacking distance, and the charge transport properties of polymers. They found that polymer with branching at 4-position (**38c**) showed the shortest $\pi–\pi$ distance at 3.57 Å and the highest hole mobility at $3.62\,\mathrm{cm^2\,V^{-1}\,s^{-1}}$ [122]. By changing the alkyl side chains to siloxane-containing side chains, Bao and coworkers obtained polymer with hole mobility near $2.48\,\mathrm{cm^2\,V^{-1}\,s^{-1}}$ [123]. More recently, the same group used the siloxane-containing polymer PII2T-Si (**38e**) to fabricate a flexible piezoelectric transistor that showed high pressure sensitivity (max. $8.4\,\mathrm{kPa^{-1}}$), fast response time (<10 ms), high stability (>15 000 cycles), and low power consumption (<1 mW) to be applied for electronic skin [124].
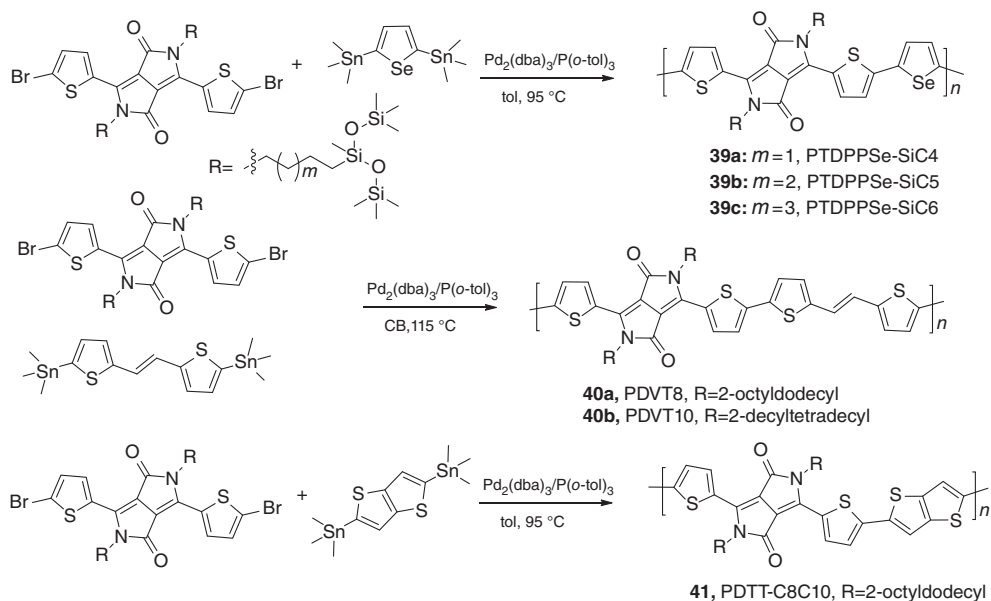
Recently, the diketopyrrolopyrrole (DPP) monomer has attracted much interest for use in high-performance FET polymers. For example, by incorporating siloxane side chains, Yang and Oh made a DPP-selenophene conjugated polymer (**39c**, Scheme 1.37), which showed ambipolar charge transport properties with a hole mobility of $3.97\,\mathrm{cm^2\,V^{-1}\,s^{-1}}$ and an electron mobility of $2.20\,\mathrm{cm^2\,V^{-1}\,s^{-1}}$ [125]. With shorter siloxane side chains, denser molecular packing and shorter $\pi–\pi$ stacking distances were observed. The best results were obtained from **39b** with hole mobility of $8.84\,\mathrm{cm^2\,V^{-1}\,s^{-1}}$ and electron mobility of $4.34\,\mathrm{cm^2\,V^{-1}\,s^{-1}}$ [126]. High mobilities can also be achieved using DPP monomer and different thiophene derivatives as

Me$_3$Sn—[thiophene]—SnMe$_3$

+

R—[thiophene]—Br / Br—[thiophene]—R

$\xrightarrow[\text{140 °C/2 min}\ \text{160 °C/2 min}\ \text{180 °C/15 min}]{\text{Pd}_2\text{(dba)}_3/\text{P(o-tol)}_3}$ CB, MW,

R—[thiophene]—R

36, PBTTT,

R = C$_{10}$H$_{21}$, C$_{12}$H$_{25}$C$_{14}$H$_{29}$

Me$_3$Sn—[thiophene]—SnMe$_3$ (R$_1$)

+

Br—[thiophene]—Br (R$_2$)

$\xrightarrow[\text{CB, 120 °C, 2 d}]{\text{Pd}_2\text{(dba)}_3/\text{P(o-tol)}_3}$

R$_1$, R$_2$ polymer

37a, PC6TV12T, R$_1$ = n-C$_6$H$_{13}$, R$_2$ = n-C$_{12}$H$_{25}$
37b, PC12TV12T, R$_1$ = R$_2$ = n-C$_{12}$H$_{25}$

Scheme 1.35 Some polythiophene derivatives for OFETs [119, 120].

38a, IIDDT: R=2-octyldodecyl
38b, IIDDT-C2: $m=2$
38c, IIDDT-C3: $m=3$
38d, IIDDT-C4: $m=4$

38e, PII2T-Si

Pd$_2$(dba)$_3$/P(o-tol)$_3$
tol, 110 °C

Pd$_2$(dba)$_3$/P(o-tol)$_3$
tol, MW 110–135 °C

Scheme 1.36 Some IID-based polymers for OFETs [121–123].

Scheme 1.37 DPP-based polymers for OFETs [117, 125–127].

comonomers, such as PDVT-C10 (**40b**) with a hole mobility of 8.3 cm^2 V^{-1} s^{-1} [127] and PDTT-C8C10 (**41**) with a hole mobility of 10.5 cm^2 V^{-1} s^{-1} at ambient conditions [117]. Interestingly, **41** showed ambipolar mobilities under vacuum. The hole mobility increased to 13.41 cm^2 V^{-1} s^{-1}, and the electron mobility became significant, reaching 1.58 cm^2 V^{-1} s^{-1}.

1.4.4 Organic Light-Emitting Diode (OLED) Polymers

1.4.4.1 Background

The electroluminescence (EL) of organic small molecular materials was first observed in 1963 in anthracene crystals [128]. Currently one step ahead of other organic electronic materials, OLED materials are the basis for displays in some of the first commercial devices, from companies such as Samsung, LG, and Sony. Universal Display Corporation holds most of the patents related to the commercialization of OLEDs. In recent years, OLEDs have improved significantly, including better efficiency, higher brightness, and lower driving voltage, which help to realize high-efficiency full color and white-color OLEDs [129].

The simplest device structure for OLEDs may consist of an emitter layer situated between two electrodes. Under an applied electric field, electrons and holes are injected from the electrodes into the active material to form excitons (bound electron–hole pairs), which then undergo recombination to excited states. Radiative emission from the excited states generates photons, which are observed as visible light if the wavelength is within the visible spectrum. However, in order to obtain high efficiency and light output, balanced electron and hole injection/transport from the cathodes and anodes is essential. Therefore, a multilayer architecture is commonly used, including a transparent and conductive indium tin oxide (ITO) anode, a hole transporting/injection layer

(HTL), an emissive layer (EML), an electron transporting/injection layer (ETL), and a metal cathode (e.g., Al) [129].

Most OLED materials have fluorescent emission, the theoretical maximum efficiency of which is 25% due to the ratio of singlet to triplet is $1:3$ in the generated excited states [128]. Some compounds, such as *fac*-tris(2-phenylpyridine)iridium (Ir(ppy)$_3$), have phosphorescent emission, thus leading to an efficiency limit of 75%. While the development of new conjugated materials can tune the emission color, electron affinity, and charge mobility of the OLED, performance optimization largely relies on proper energy-level matching between active materials, charge transport layers, and electrodes. The main parameter used to represent the efficiency of OLEDs is EQE, which is the ratio of the emitted photons over the charges injected into the material.

Conjugated polymer-based organic light-emitting diode (P-OLED) materials were first reported in PPV materials in 1990 [130]. Since then, they have been rapidly improving, somewhat due to the versatility offered by the Stille polycondensation. Careful selection of reaction conditions and purification processes is essential for OLED polymers, because even small amounts of impurities or unreacted functional groups such as halide can quench the fluorescence [128]. As such, the Stille coupling method is one of the effective methods to produce high-quality, high-performance polymers easily. Typical conditions for Stille polycondensation for producing other organic semiconducting materials, including OPVs and OFETs, are also viable for P-OLEDs.

1.4.4.2 Examples of OLED Polymers Synthesized by Stille Polycondensation

A thorough investigation on the synthesis of conjugated polymers for EL applications can be found in the review by Holmes and coworkers [128]. Here, we will provide some examples of P-OLED materials that are synthesized by Stille polycondensation.

PPV is a widely studied and good material for P-OLEDs. It is normally deposited as soluble precursors onto metal electrodes and then converted into the final polymer by thermal decomposition or photoirradiation, because the nonsubstituted PPV is barely soluble in common organic solvents [128]. However, with solubilizing side chains, PPV derivatives can be easily prepared via Stille polycondensation. For example, Babudri *et al.* prepared a PPV polymer with alkoxy side chains from 1,4-diiodo-2,5-dipentyloxybenzene and *trans*-1,2-bis(tributylstannyl)ethene, using Pd catalyst in benzene solvent (**42**, Scheme 1.38) [131]. Different Pd catalysts, including Pd(PPh$_3$)$_4$, Pd(PPh$_3$)$_2$Cl$_2$, and Pd(OAc)$_2$, gave the resulting polymer with M_n 2.0–2.5 kDa and dispersity 1.5–1.6. Note that with DMF solvent, poor results were obtained.

Cao and coworkers [132] synthesized another series of alkoxy PPV polymers via Stille polycondensation in a mixed solvent system of toluene:DMF $= 2:1$. The resulting polymers (**43**, Scheme 1.38) showed relatively low molecular weight ($M_n \sim 5$ kDa) and wide dispersity (Đ $\sim$3). Compound **43** showed EL $\lambda_{max} = 591$ nm with a luminance of 61 cd m^{-2} and an EQE of 0.17%. Incorporation of the BT unit (**44**, Scheme 1.39) decreased luminance and significantly red-shifted the EL λ_{max} from 591 nm to between 659 and 724 nm, depending on different proportions of BT component. The random copolymer **36** was a deep and exclusively red-emitting material when fabricated in a device structure of ITO/PEDOT:PSS/polymer/Ba/Al. The same group also made similar polymers with reported near-IR emission by incorporating BT or benzoselenadiazole
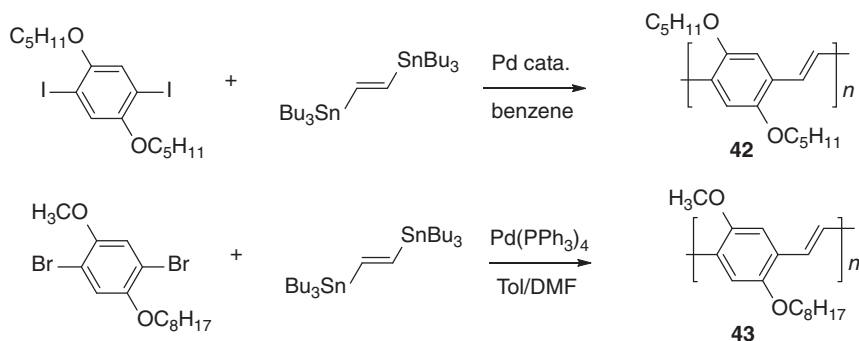
Scheme 1.38 Synthesis of soluble PPV derivatives [131, 132].
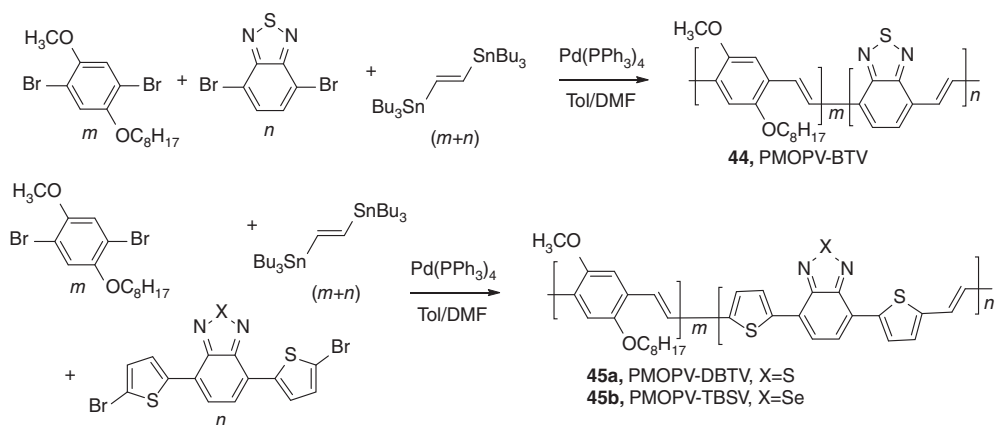
Scheme 1.39 Synthesis of PPV-based random copolymers for P-OLED [132, 133].

units (**45**, Scheme 1.39) [133]. The EL λ_{max} was further shifted to as far as 762 for **45a** with 30% DBTV and 800 nm for **45b** with 30% TBSV. The highest EQE for **45a** reached 0.31% with 1% DBTV, and for **45b** 0.16% with 1% TBSV.

Pyridine derivatives are also useful in preparing P-OLEDs. Register and coworkers synthesized several poly(pyridyl vinylene) (PPyV, **46**) polymers and their pyridium forms with different alkyl chains (Scheme 1.40) [134]. A PPV hole transporting layer improved the carrier injection into Bu-PPyV, leading to an enhanced EQE from 0.02% to 0.05% in an LED device of ITO/PPV/Bu-PPyV/Al. In another report, Onoda and coworkers achieved a maximum EQE of 0.08% with orange-red EL $\lambda_{max} = 585$ nm from PPyV [135]. Due to the asymmetric nature of pyridine, PPyV can have three regioisomers: head-to-head (HH, **47b**), head-to-tail (HT, **47c**), and random (R, **47a**). Swager and coworkers prepared these three regioisomers according to different synthetic approaches (Scheme 1.41) [136]. Both the random and HH PPyV were synthesized by Stille polycondensation, while HT PPyV by Heck polycondensation. The key steps for HH or HT polymers were the preparation of relative HH or HT precursors. The HH and HT PPyV showed red-shifted absorption and emission spectra comparing to random version, with EL λ_{max} at 575 nm (R), 584 nm (HT), and 605 nm (HH), indicating longer effective conjugation lengths in the regioregular isomers [128].
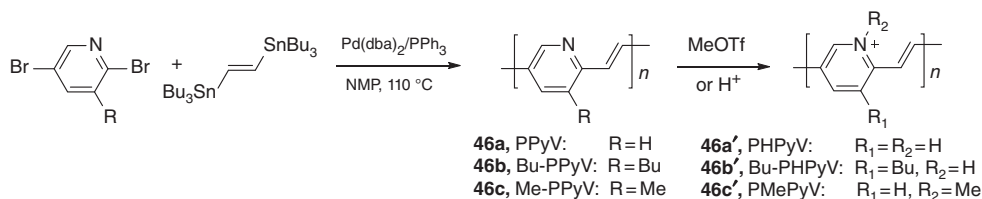
**Scheme 1.40** Synthesis of PPyV polymers and their pyridinium forms [134].

Stille polycondensation is also an effective method to prepare many thiophene-based conjugated polymers for P-OLEDs. Moreau and coworkers prepared a regioregular (>95% HT) poly(alkylthiophene) and poly(alkylbithiophene) via Stille coupling from bifunctional mono−bromo−mono−tin compounds (Scheme 1.42) [137]. High molecular weights and low dispersities were obtained for them (**48a**: $M_n = 142.02$ kDa, Đ = 1.5; **48b**: $M_n = 34$ kDa, Đ = 1.1). This regioregular polymer showed a red shift in the ultraviolet (UV)−visible spectrum compared to their regiorandom counterparts both in solution and in film state. The authors also examined various Pd catalysts and reported the best results with 0.5 mol% of $Pd_2(dba)_3(CHCl_3)$ and 4% of PPh_3 in THF/DMF(1:1) at 80 °C, heating for 72 h. Melucci and coworkers reported the synthesis of a V-shaped conjugated polymer from a bithiophene monomer and a thiophene sulfone monomer via Stille polycondensation with in situ generated $Pd(AsPh_3)_4$ from $Pd_2(dba)_3$ and $AsPh_3$ (Scheme 1.43) [138]. However, according to its molecular weight ($M_n = 1.1$ kDa, Đ = 1.39), **49** was an oligomer rather than a polymer. Though its PL efficiency was low at 1−2%, it showed orange-red emission (EL $\lambda_{max} = 625$ nm) and a very high luminance of 948 cd m^{-2} on a single-layered LED device.

CPDTs with different bridging atoms are important thiophene derivatives, which have also been reported as building blocks for P-OLED materials. For example, Ohshita and coworkers reported the synthesis of conjugated polymers from dithiophenesilole monomers and oligothiophene monomers (**50**, Scheme 1.44) [139]. A Stille condition with $CuCl_2$ additive in THF at 0 °C gave the optimal results. The polymer showed yellow emission (EL $\lambda_{max} = 592$ nm) and an LED device of ITO/polymer/Alq$_3$/Mg-Ag showed high luminance of 500 cd m^{-2} at 13 V. Alq$_3$ is tris(8-quinolinolato)aluminum(III), a vapor-deposited electron-transporting layer. Patri and coworkers reported a dithiophenepyrrole containing polymer (**51**, Scheme 1.44) [140]. The use of CuO additive enabled high molecular weight of the resulting polymer ($M_n \sim 50$ kDa). These polymers exhibited red emission with EL ranging from 780 to 814 nm, depending on the different alkyl chains. With a structure of ITO/PEDOT:PSS/Polymer/BCP/Alq$_3$/LiF/Al, the LED devices of the polymers displayed low threshold voltage (3−4 V) and the maximum luminance for **51c** was observed to be 54 cd m^{-2} at 9 V.

1.4.5 Other Functional Materials

While the family of functional materials is large and a tremendous amount of them is synthesized by Stille polycondensation, we have only covered the main classes of materials so far. In addition to this, conjugated polymers find use in a number of other niche applications. The following are some functional materials with different applications.
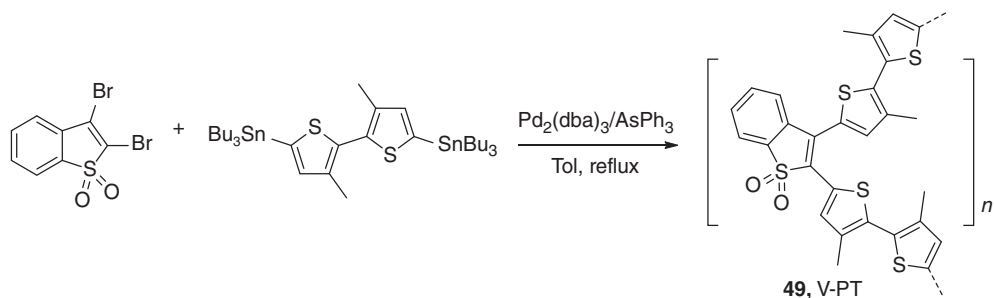
Conjugated polymers are widely used for sensor materials, since they can exhibit significant and reproducible properties such as luminescence and conductivity, which are
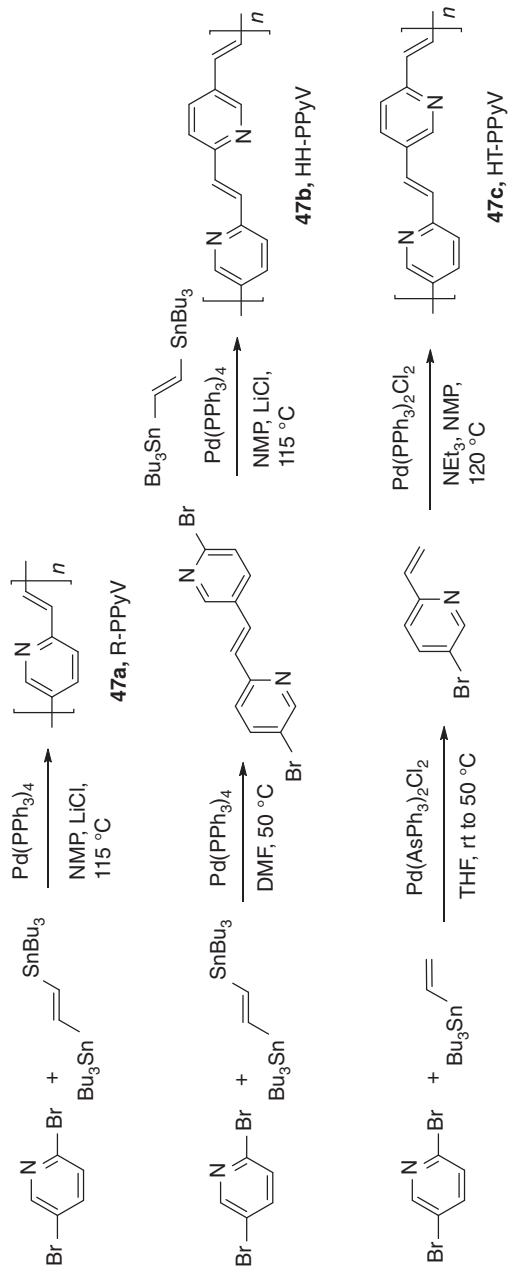
**Scheme 1.41** Synthesis of random and regioregular PPyV polymers [136].
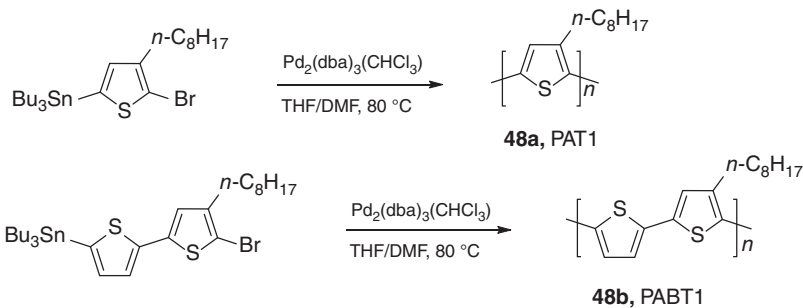
Scheme 1.42 Synthesis of regioregular polythiophenes using Stille method [137].


Scheme 1.43 Synthesis of V-shaped polythiophene V-PT [138].

sensitive to minor perturbations in their environment. Attaching analyzing units into the polymer is generally adopted to make materials for chemical sensors and biosensors, which respond to specific analytes, such as nucleotides, metal ions, and other environmental factors. For example, **52** and **53** (Scheme 1.45), which had polythiophene backbones and were synthesized via electrochemical polymerization, were capable of binding of purine or pyrimidine through hydrogen bonds, enabling them to detect small concentrations of purine or pyrimidine due to changes in the oxidation potential and electroactivity of the polymer [141–143]. Swager and coworkers synthesized a series of polythiophene-based sensor polymers by Stille polycondensation (**54**, Scheme 1.46) [144]. The chelating cyclophane receptor side chains grafted onto the polymer backbone could form pseudorotaxane complexes with trace amount of metal ions, inducing a decrease in carrier mobility and conductivity, with other voltammetric, chromic, fluorescent, and resistive responses.

LCs are an important class of functional materials that have properties between those of a liquid and a solid. An LC may flow like a liquid, but its molecules may order like a crystal, which can be observed by polarizing optical microscopy. LC materials are widely used in modern electronic display technologies. Some conjugated polymers can also be designed as LC materials, proving good processability, together with various optical and electronic properties. Yu and coworkers have developed a series of PPT polymers that exhibited nematic LC phases (**1**, Scheme 1.4). By changing the length of the side chains, one can optimize the physical properties of the resulting polymers, such as transition temperatures, solubility, and fusibility. For example, Goto and coworkers synthesized a series of phenylene–thiophene-based conjugated polymers bearing pyrimidine LC
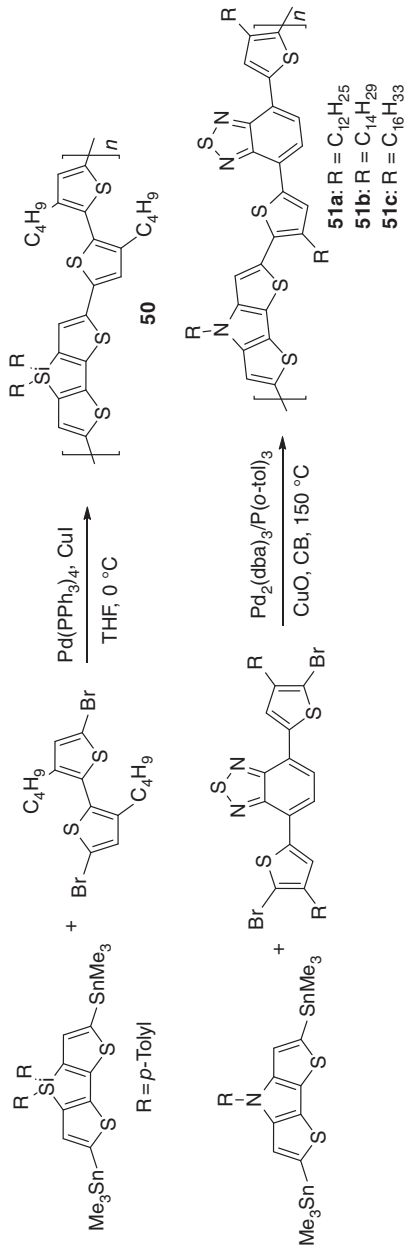
Scheme 1.44 Synthesis of some OFET polymers based on CPDT with different bridging atoms [139, 140].
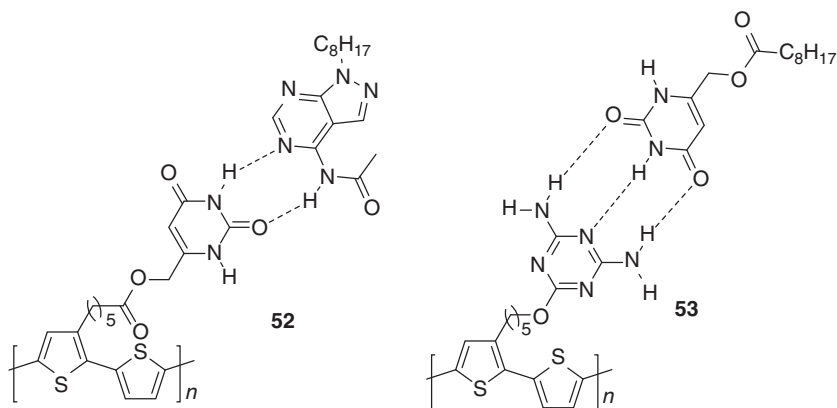
Scheme 1.45 Examples of polythiophenes that can detect purine and pyrimidine via H-bonds [141–143].

moieties via Stille polycondensation (**55**, Scheme 1.47) [145]. The resulting polymers exhibited a nematic LC mesophase at appropriate temperatures. Another interesting property was the generation of radical cations on the polymer (polarons) by in situ vapor doping of iodine, which indicated that the polymers may be potentially applied as a conductive LC material [145].

In recent years, some hybrid organic–inorganic materials have attracted significant interest as functional materials. One important class of these is metal-containing polymers, especially those with precious metals such as iridium and platinum. These heavy metal atoms form an integral part of the backbone or side chains of the polymers, wherein their mixing of singlet and triplet excited states, high phosphorescence yields, and relatively long emission lifetimes make the resulting polymers attractive for opto-electronic applications. Many different synthetic methods are utilized to synthesize these metal-containing polymers [146], including Stille polycondensation.

## 1.5 Challenge and Outlook

1.5.1 Advantages of the Stille Reaction

As discussed above, the major advantages of the Stille coupling reaction are that it requires mild reaction conditions, can tolerate diverse functional groups, and is stereo- and regio-selective. These advantages make this methodology useful for the synthesis of functional polymeric materials in that it is possible to design materials with different functional units to exhibit desirable properties. The preparation of the starting monomers is facile for both the organostannane and electrophile. They are often synthesized straightforwardly and can be functionalized intentionally. In addition, the organostannane is normally quite stable against oxygen and moisture, and thus easier to handle, unlike some other organometallic compounds such as Grignard reagents (for Kumada coupling) or organozinc reagents (for Negishi coupling).

Furthermore, its versatility provides a unique approach to the synthesis of complex compounds that bear sensitive functional groups. For example, the key steps in the
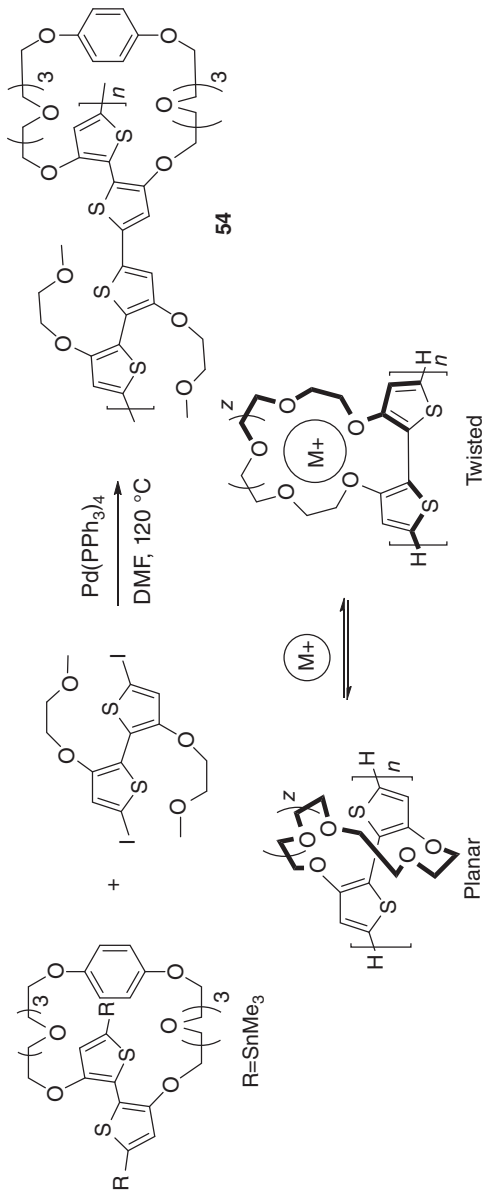
Scheme 1.46 Synthesis of polythiophene sensor polymer and its interaction with metal ions [144].
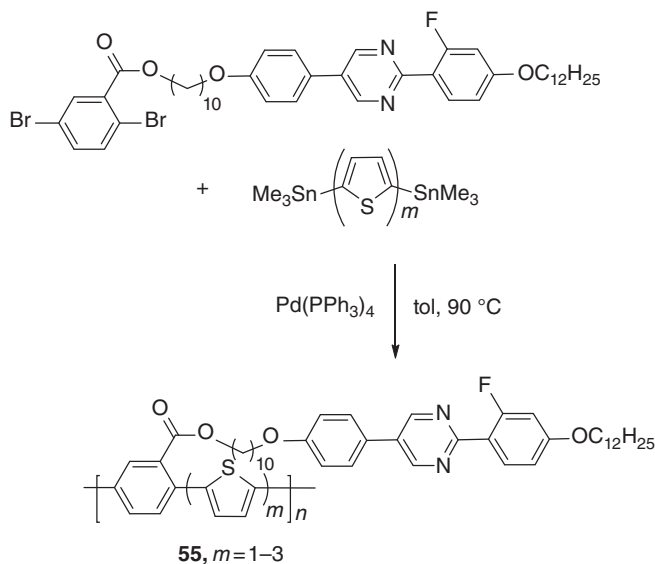
**Scheme 1.47** Synthesis of phenylene–thiophene-based liquid crystal polymer.

total synthesis of macrocycle compounds such as rapamycin by Nicolaou *et al.* [147] and dynemicin A by Danishefsky *et al.* [148] involved a Stille reaction between 1,2-bis(tributylstannous)ethane and relative diiodo compounds (Scheme 1.48).

Compared to the Stille polycondensation, other Pd-catalyzed coupling reactions have significant limitations for synthesizing functional materials. For example, the Suzuki cross-coupling reaction between organoboranes and electrophiles has a few major drawbacks (Scheme 1.49). The foremost is the requirement of basic reaction conditions. As a result, monomers with functional groups that are labile under basic conditions are not suitable for this reaction, unless additional protecting strategies are used. Also, the Suzuki coupling reaction needs polar solvents and sometimes even a biphasic mixture. This may decrease the solubility of polymers, especially as the molecular weight increases, and thus lead to low molecular weights and high dispersity for the polymers [7].

Another competing cross-coupling reaction, Kumada coupling (Scheme 1.50) represents a successful method to make homopolymers such as polythiophenes. In 1980, Yamamoto and coworkers used an analog of Kumada coupling to make polythiophene by the reaction of 2,5-dibromothiophene with magnesium in THF in the presence of a nickel catalyst [149]. This was viewed as the first example of the planed synthesis of polythiophene. In 1992, McCullough and coworkers synthesized the first regioregular poly(3-alkylthiophene) using Kumada coupling [70]. However, this approach will encounter difficulty when a monomer sensitive to nucleophilic attack by Grignard reagents, limiting its scope.

1.5.2 Disadvantages of Stille Reaction

Though efficient in synthetic applications, the Stille polycondensation also has some disadvantages. The biggest challenge involves the toxicity of organostannane
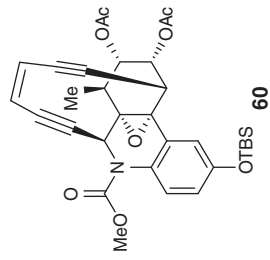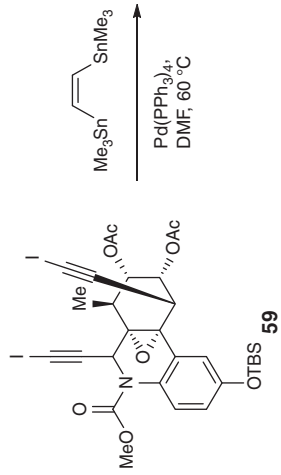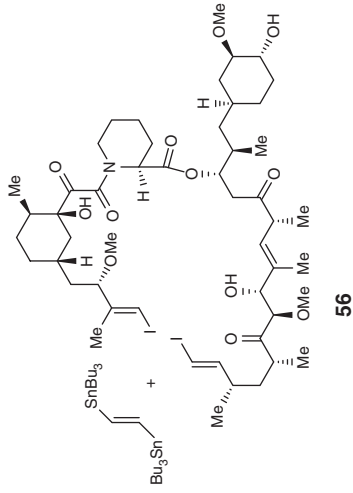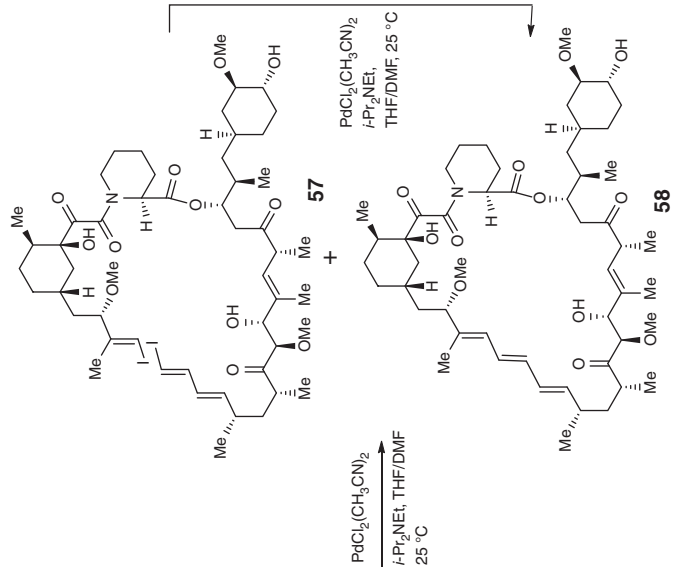
Scheme 1.48 Stille coupling in the total synthesis of rapamycin and dynemicin A [147, 148].

$$\text{Ar}_1\text{—B(OR)}_2 \;+\; \text{Ar}_2\text{—X} \quad \xrightarrow[\text{Base}]{\text{Pd cata.}} \quad \text{Ar}_1\text{–Ar}_2 \;+\; \text{X-B(OR)}_2$$
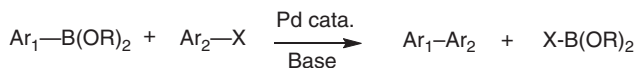
Scheme 1.49 Reaction scheme of Suzuki coupling for conjugated polymers.

$$\text{R}_1\text{-MgX} \;+\; \text{R}_2\text{-X} \quad \xrightarrow{\text{Ni or Pd cata.}} \quad \text{R}_1\text{–R}_2$$

$\quad$ R_1= alkyl, vinyl, aryl
$\quad$ R_2= vinyl, aryl

Scheme 1.50 Reaction scheme for Kumada coupling.

monomers, and may potentially cause the environmental, health, and safety issues. A typical synthesis of the ditin monomers involves the use of tin source, such as tri-*n*-butyltin chloride or trimethyltin chlorid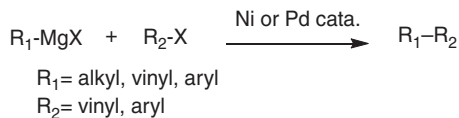e, and an organolithium reagent, such as *n*-butyllium or lithium diisopropylamine (LDA). Although the toxicity and volatility of tri-*n*-butyltin ($LD_{50} = 100 - 300 \, \text{mg kg}^{-1}$) are lower than that of the trimethyltin ($LD_{50} < 15 \, \text{mg kg}^{-1}$) [20], tri-*n*-butyltin compounds are more difficult to purify via recrystallization. Improper handling and disposure of these tin-containing compounds could cause heavy metal pollution and be harmful to human health. In addition, many tin compounds are still too labile to be purified; impure monomers will hinder the synthesis of polymers with high molecular weight. In addition, the remaining tin in the final product is difficult to remove completely even with the treatment of KF aqueous solution.

Another issue is the phosphine ligand used in the catalytic system. They are normally sensitive to moisture and air, expensive, and toxic, though not as toxic as the organotin compounds. This is especially true for the more specialized phosphines used for the coupling of aryl chlorides, which are cheaper but less reactive than bromide and iodide counterparts. Finally, side reactions are known which incorporate phosphines into the backbone of conjugated polymers in some cases, though these reactions are rare.

Several approaches have been considered to make the Stille reaction greener: (i) catalytic use of stannanes, (ii) use polymer-immobilized stannanes, (iii) ionic liquid-supported and phosphonium-supported Stille reactions, and (iv) use recyclable or less toxic molecular stannanes [20]. For example, Maleczka and coworkers reported the catalytic use of tin in the reaction of halides with alkyne, which reacted with Bu_3SnH to produce vinyl tin, then underwent Stille catalytic cycle [150, 151]. The use of polymethylhydrosiloxane (PMHS) enabled the regeneration of Bu_3SnH from the coupling product Bu_3SnX through a "Si-F" or "Si-O" approach (Scheme 1.51). Though the reaction scope was limited to vinyl substrates, it provided an interesting possibility. Moreover, Legoupy and coworkers reported an ionic liquid-supported Stille reaction (Scheme 1.52) [152]. The organotin compounds could be recycled via the corresponding Grignard reagents and the contamination of tin was very low ([Sn] < 3 ppm), as determined by Inductively coupled plasma-mass spectrometry. Notably, the reaction could be carried out without the need for solvent, ligand, or additives, offering a green approach to the Stille reaction.

Further, though the reaction conditions of the Stille reaction itself can tolerate a wide variety of functional groups, synthesis of the ditin monomers themselves may have more
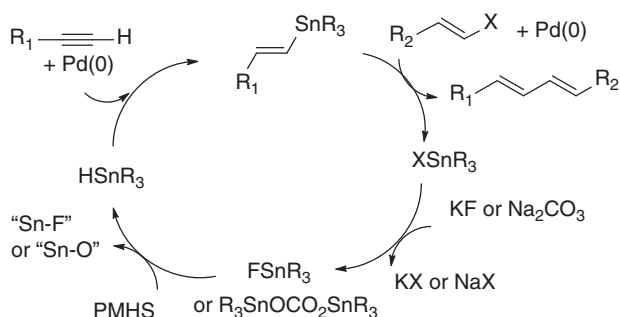
Scheme 1.51 Catalytic use of tin in Stille coupling [150, 151].

R_1 = allyl, vinyl, Ar; R_2 = Ar
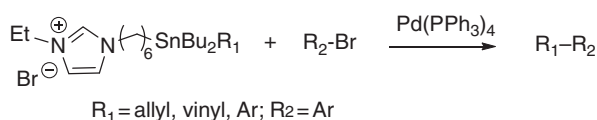
Scheme 1.52 Ionic liquid supported Stille coupling [152].

stringent functional group requirements, because organometallic compounds are usually used to prepare ditin monomers, which may limit the choice of functional groups in the ditin monomers.

Another issue about the Stille polycondensation concerns the stoichiometry. Precise stoichiometric balance is essential to achieve high molecular weights in polymers. Thus, monomers with high purity are needed, which requires additional work on the purification process. However, even with very pure monomers, the nature of the Stille coupling may interfere with the stoichiometric balance. Some monomers may undergo homocoupling instead of cross-coupling (see Section 4.2). It was shown that the homocoupling by-product might act as defects in the polymer chains, which may result in detrimental effects on the desired physical properties [153].

In addition, the palladium black formed during the polymerization needs to be removed since it is known to interfere with the electronic properties of the final polymers. Though effective, the typically used purification method of filtration over Celite is not sufficient to fully remove trace amount of palladium metal particles. Thus, new methods have been reported using strong chelating reagents to remove palladium [7, 84]. However, this might also introduce additional impurities to the final polymers.

1.6 Summary

In summary, tremendous progress has been made toward understanding the mechanism of the Stille reaction and optimizing the reaction conditions, and using it as a powerful method to synthesize various functional organic compounds. Typically involving organostannanes and organohalides or pseudohalides as the coupling counterparts, this methodology has the advantages of mild reaction conditions, and thus tolerance toward a wide range of functional groups, and high reactivity. A wide range of functional materials, including various optical and electronic materials, as well as chemical and biosensors, as discussed above, have been synthesized and developed over the past

several decades. The Stille polycondensation reaction is now an indispensable synthetic approach to various new functional materials. Yet this methodology is not perfect and has its disadvantages, such as the toxicity of tin reagent, difficulty in purification of the tin monomers, use of expensive palladium catalysts, and side reactions involving homo-coupling by-products. Thus, further development of this polycondensation reaction and the search for alternative approaches, which use nontoxic monomers, are desirable. One new direction will be to study the use of Pd-mediated coupling reactions involving C–H bond activation for the synthesis of functional polymers. On the basis of these discussions, we can conclude that the future is full of challenging issues, but bright as efforts are made to tackle them and make this method greener and more efficient.

References

1 Muller, T.J.J. and Bunz, U.H.F. (2007) *Functional Organic Materials: Synthe-ses, Strategies and Applications*, 1st edn, Wiley-VCH Verlag GmbH. ISBN: 9783527313020

2 Sinn, H. and Kaminsky, W. (1980) Ziegler-Natta catalysis. *Adv. Organomet. Chem.*, **18**, 99–149.

3 Coates, G.W., Hustad, P.D., and Reinartz, S. (2002) Catalysts for the living inser-tion polymerization of alkenes: access to new polyolefin architectures using Ziegler-Natta chemistry. *Angew. Chem. Int. Ed.*, **41**, 2236–2257.

4 Miyaura, N. and Suzuki, A. (1995) Palladium-catalyzed cross-coupling reactions of organoboron compounds. *Chem. Rev.*, **95**, 2457–2483.

5 Beletskaya, I.P. and Cheprakov, A.V. (2000) The Heck reaction as a sharpening stone of palladium catalysis. *Chem. Rev.*, **100**, 3009–3066.

6 Corbet, J.-P. and Mignani, G. (2006) Selected patented cross-coupling reaction technologies. *Chem. Rev.*, **106**, 2651–2710.

7 Carsten, B., He, F., Son, H.J., Xu, T., and Yu, L. (2011) Stille polycondensation for synthesis of functional materials. *Chem. Rev.*, **111**, 1493–1528.

8 Gunes, S., Neugebauer, H., and Sariciftci, N.S. (2007) Conjugated polymer-based organic solar cells. *Chem. Rev.*, **107**, 1324–1338.

9 Azarian, D., Dua, S.S., Eaborn, C., and Walton, D.R.M. (1976) Reaction of organic halides with R_3MMR_3 compounds (M = Si, Ge, Sn) in the presence of Tetrakis(triarylphosphine) palladium. *J. Organomet. Chem.*, **117**, C55–C57.

10 Kosugi, M., Shimizu, Y., and Migita, T. (1977) Reaction of allyltin compounds II. Facile preparation of allyl ketones via allyltins. *J. Organomet. Chem.*, **129**, C36–C38.

11 Kosugi, M., Shimizu, Y., and Migita, T. (1977) Alkylation, arylation, and vinylation of acyl cglorides by means of organotin compounds in the presence of catalytic amounts of tetrakis (triphenylphosphine)palladium(0). *Chem. Lett.*, **6**, 1423–1424.

12 Kosugi, M., Sasazawa, K., Shimizu, Y., and Migita, T. (1977) Reactions of allyltin compounds III allylation of aromatin halided with allyltributyltin in the presence of tetrakis(triphenyl phosphine)palladium(0). *Chem. Lett.*, **6**, 301–302.

13 Milstein, D. and Stille, J.K. (1978) A general, selective, and facile method for ketone synthesis from acid chlorides and organotin compounds catalyzed by palladium. *J. Am. Chem. Soc.*, **100**, 3636–3638.

14 Milstein, D. and Stille, J.K. (1979) Palladium-catalyzed coupling of tetraorganotin compounds with aryl and benzyl halides. Synthetic utility and mechanism. *J. Am. Chem. Soc.*, **101**, 4992–4998.

15 Stille, J.K. (1986) The palladium-catalyzed cross-coupling reactions of organotin reagents with organic electrophiles. *Angew. Chem. Int. Ed. Engl.*, **25**, 508–524.

16 Bao, Z., Chan, W.-K., and Yu, L. (1993) Synthesis of conjugated polymer by the Stille coupling reaction. *Chem. Mater.*, **5**, 2–3.

17 Yu, L., Bao, Z., and Cai, R. (1993) Conjugated, liquid crystalline polymers. *Angew. Chem. Int. Ed. Engl.*, **32**, 1345–1347.

18 Bao, Z., Chan, W.-K., and Yu, L. (1995) Exploration of the Stille coupling reaction for the syntheses of functional polymers. *J. Am. Chem. Soc.*, **117**, 12426–12435.

19 Espinet, P. and Echavarren, A.M. (2004) The mechanisms of the Stille reaction. *Angew. Chem. Int. Ed.*, **43**, 4704–4734.

20 Cordovilla, C., Bartolomé, C., Martínez-Ilarduya, J.M., and Espinet, P. (2015) The Stille reaction, 38 years later. *ACS Catal.*, **5**, 3040–3053.

21 Casado, A.L. and Espinet, P. (1998) On the configuration resulting from oxidative addition of RX to $Pd(PPh_3)_4$ and the mechanism of the cis-to-trans isomerization of $[PdRX(PPh_3)_2]$ complexes (R = Aryl, X = Halide). *Organometallics*, **17**, 954–959.

22 Portnoy, M. and Milstein, D. (1993) Mechanism of aryl chloride oxidative addition to chelated palladium(0) complexes. *Organometallics*, **12**, 1665–1673.

23 Farina, V. and Roth, G.P. (1996) Recent avances in the Stille reaction. *Adv. Met. Org. Chem.*, **5**, 1–53.

24 Farina, V. (1996) New perspectives in the cross-coupling reactions of organostannanes. *Pure Appl. Chem.*, **68**, 73–78.

25 Amatore, C., Bahsoun, A.A., Jutand, A., Meyer, G., Ndedi Ntepe, A., and Ricard, L. (2003) Mechanism of the Stille reaction catalyzed by palladium ligated to arsine ligand: $PhPdI(AsPh_3)(DMF)$ is the species reacting with vinylstannane in DMF. *J. Am. Chem. Soc.*, **125**, 4212–4222.

26 Casado, A.L., Espinet, P., and Gallego, A.M. (2000) Mechanism of the Stille reaction. 2. Couplings of aryl triflates with vinyltributyltin. Observation of intermediates. A more comprehensive scheme. *J. Am. Chem. Soc.*, **122**, 11771–11782.

27 Casado, A.L. and Espinet, P. (1998) Mechanism of the Stille reaction. 1. The transmetalation step. Coupling of R^1I and R^2SnBu_3 catalyzed by trans-$[PdR^1IL2]$ ($R^1 = C_6Cl_2F_3$; R^2 = Vinyl, 4-Methoxyphenyl; L = $AsPh_3$). *J. Am. Chem. Soc.*, **120**, 8978–8985.

28 Labadie, J.W. and Stille, J.K. (1983) Mechanisms of the palladium-catalyzed couplings of acid chlorides with organotin reagents. *J. Am. Chem. Soc.*, **105**, 6129–6137.

29 Louie, J. and Hartwig, J.F. (1995) Transmetalation involving organotin aryl, thiolate, and amide compounds. An unusual type of dissociative ligand substitution reaction. *J. Am. Chem. Soc.*, **117**, 11598–11599.

30 Albeniz, A.C., Espinet, P., and Martin-Ruiz, B. (2001) The Pd-catalyzed coupling of allyl halides and tin aryls: why the catalyc reaction works and the stoishiometric reaction does not. *Chem. Eur. J.*, **7**, 2481–2489.

31 Fu, G.C. (2008) The development of versatile methods for palladium-catalyzed coupling reactions of aryl electrophiles through the use of $P(t-Bu)_3$ and PCy_3 as ligands. *Acc. Chem. Res.*, **41**, 1555–1564.

32 Calo, V., Nacci, A., Monopoli, A., and Montingelli, F. (2005) Pd nanoparticles as efficient catalysts for Suzuki and Stille coupling reactions of aryl halides in ionic liquids. *J. Org. Chem.*, **70**, 6040–6044.

33 Amatore, C., Carre, E., Jutand, A., and M'Barki, M.A. (1995) Rates and mechanism of the formation of zerovalent palladium complexes from mixtures of Pd(OAc)2 and tertiary phosphines and their reactivity in oxidative additions. *Organometallics*, **14**, 1818–1826.

34 Doucet, H., Ohkuma, T., Murata, K., Yokozawa, T., Kozawa, M., Katayama, E., England, A.F., Ikariya, T., and Noyori, R. (1998) trans-[RuCl2(phosphane)2(1,2-diamine)] and chiral trans-[RuCl2(diphosphane)(1,2-diamine)]: shelf-stable precatalysts for the rapid, productive, and stereoselective hydrogenation of ketones. *Angew. Chem. Int. Ed. Engl.*, **37**, 1703–1707.

35 Strieter, E.R., Blackmond, D.G., and Buchwald, S.L. (2003) Insights into the origin of high activity and stability of catalysts derived from bulky, electron-rich monophosphinobiaryl ligands in the Pd-catalyzed C-N bond formation. *J. Am. Chem. Soc.*, **125**, 13978–13980.

36 Su, W., Urgaonkar, S., McLaughlin, P.A., and Verkade, J.G. (2004) Highly active palladium catalysts supported by bulky proazaphosphatrane ligands for Stille cross-coupling: coupling of aryl and vinyl chlorides, room temperature coupling of aryl bromides, coupling of aryl triflates, and synthesis of sterically hindered biaryls. *J. Am. Chem. Soc.*, **126**, 16433–16439.

37 Littke, A.F., Schwarz, L., and Fu, G.C. (2002) Pd/P(-Bu)$_3$: a mild and general catalyst for Stille reactions of aryl chlorides and aryl bromides. *J. Am. Chem. Soc.*, **124**, 6343–6348.

38 Amatore, C., Bucaille, A., Fuxa, A., Jutand, A., Meyer, G., and Ndedi Ntepe, A. (2001) Rate and mechanism of the oxidative addition of phenyl iodide to Pd0 ligated by triphenylarsine: evidence for the formation of a T-shaped complex [PhPdI(AsPh$_3$)] and for the decelerating effect of CH$_2$=CH–SnBu$_3$ by formation of [Pd$_0$(η^2-CH$_2$=CH–SnBu$_3$)(AsPh$_3$)$_2$]. *Chem. Eur. J.*, **7**, 2134–2142.

39 Farina, V. and Krishnan, B. (1991) Large rate accelerations in the Stille reaction with Tri-2-furylphosphine and triphenylarsine as palladium ligands: mechanistic and synthetic implications. *J. Am. Chem. Soc.*, **113**, 9585–9595.

40 Labadie, J.W. and Stille, J.K. (1983) Stereochemistry of transmetalation in the palladium-catalyzed coupling of acid chlorides and organotins. *J. Am. Chem. Soc.*, **105**, 669–670.

41 Malova Krizkova, P. and Hammerschmidt, F. (2013) On the configurational stability of chiral heteroatom-substituted [D]methylpalladium complexes as intermediates of Stille and Suzuki-Miyaura cross-coupling reactions. *Eur. J. Org. Chem.*, **2013**, 5143–5148.

42 Liu, Y., Zhao, J., Li, Z., Mu, C., Ma, W., Hu, H., Jiang, K., Lin, H., Ade, H., and Yan, H. (2014) Aggregation and morphology control enables multiple cases of high-efficiency polymer solar cells. *Nat. Commun.*, **5**, 5293.

43 Scott, W.,.J. and Stille, J.K. (1986) Palladium-catalyzed coupling of vinyl triflates with organostannanes. Synthetic and mechanistic studies. *J. Am. Chem. Soc.*, **108**, 3033–3040.

44 Powell, N.A. and Rychnovsky, S.D. (1996) Iodide acceleration in the Pd-catalyzed coupling of aromatic 1,2-ditriflates with alkynes: synthesis of enediynes. *Tetrahedron Lett.*, **37**, 7901–7904.

45 Roy, A.H. and Hartwig, J.F. (2003) Oxidative addition of aryl tosylates to palladium(0) and coupling of unactivated aryl tosylates at room temperature. *J. Am. Chem. Soc.*, **125**, 8704–8705.

46 Farina, V., Krishnan, B., Marshall, D.R., and Roth, G.P. (1993) Palladium-catalyzed coupling of arylstannanes with organic sulfonates: a comprehensive study. *J. Org. Chem.*, **58**, 5434–5444.

47 Menzel, K. and Fu, G.C. (2003) Room-temperature Stille cross-couplings of alkenyltin reagents and functionalized alkyl bromides that possess beta hydrogens. *J. Am. Chem. Soc.*, **125**, 3718–3719.

48 Mee, S.P., Lee, V., and Baldwin, J.E. (2005) Significant enhancement of the Stille reaction with a new combination of reagents-copper(I) iodide with cesium fluoride. *Chemistry*, **11**, 3294–3308.

49 Srogl, J., Allred, G.D., and Liebeskind, L.S. (1997) Sulfonium salts. Participants par excellence in metal-catalyzed carbon-carbon bond-forming reactions. *J. Am. Chem. Soc.*, **119**, 12376–12377.

50 Farina, V., Kapadia, S., Krishnan, B., Wang, C., and Liebeskind, L.S. (1994) On the nature of the "copper effect" in the Stille cross-coupling. *J. Org. Chem.*, **59**, 5905–5911.

51 Han, X., Stoltz, B.M., and Corey, E.J. (1999) Cuprous chloride accelerated Stille reactions. A general and effective coupling system for sterically congested substrates and for enantioselective synthesis. *J. Am. Chem. Soc.*, **121**, 7600–7605.

52 Alphonse, F.-A., Suzenet, F., Keromnes, A., Lebret, B., and Guillaumet, G. (2003) Copper(I)-promoted palladium-catalyzed cross-coupling of unsaturated tri-n-butylstannane with heteroaromatic thioether. *Org. Lett.*, **5**, 803–805.

53 Aguilar-Aguilar, A., Liebeskind, L.S., and Pena-Cabrera, E. (2007) Pd-catalyzed, Cu(I)-mediated cross-couplings of bisarylthiocyclobutenediones with boronic acids and organostannanes. *J. Org. Chem.*, **72**, 8539–8542.

54 Larhed, M. and Hallberg, A. (1996) Microwave-promoted palladium-catalyzed coupling reactions. *J. Org. Chem.*, **61**, 9582–9584.

55 Kappe, C.O. (2004) Controlled microwave heating in modern organic synthesis. *Angew. Chem. Int. Ed.*, **43**, 6250–6284.

56 Coffin, R.C., Peet, J., Rogers, J., and Bazan, G.C. (2009) Streamlined microwave-assisted preparation of narrow-bandgap conjugated polymers for high-performance bulk heterojunction solar cells. *Nat. Chem.*, **1**, 657–661.

57 Marder, S.R., Kippelen, B., Jen, A.K.-Y., and Peyghambarian, N. (1997) Design and synthesis of chromophores and polymers for electro-optic and photorefractive applications. *Nature*, **388**, 845–851.

58 Burland, D.M., Miller, R.D., and Walsh, C.A. (1994) Second-order nonlinearity in poled-polymer systems. *Chem. Rev.*, **94**, 31–75.

59 Peng, Z. and Yu, L. (1994) Second-order nonlinear optical polyimide with high-temperature stability. *Macromolecules*, **27**, 2638–2640.

60 Yu, D. and Yu, L. (1994) Design and synthesis of functionalized polyimides for second-order nonlinear optics. *Macromolecules*, **27**, 6718–6721.

61 Yu, D., Gharavi, A., and Yu, L. (1996) Highly stable copolyimides for second-order nonlinear optics. *Macromolecules*, **29**, 6139–6142.

62 Saadeh, H.A., Wang, L., and Yu, L. (2000) A new synthetic approach to novel polymers exhibiting large electrooptic coefficients and high thermal stability. *Macromolecules*, **33**, 1570–1576.

63 Babudri, F., Cardone, A., Farinola, G.M., Naso, F., Cassano, T., Chiavarone, L., and Tommasi, R. (2003) Synthesis and optical properties of a copolymer of tetrafluoro- and dialkoxy-substituted poly(p-phenylenevinylene) with a high percentage of fluorinated units. *Macromol. Chem. Phys.*, **204**, 1621–1627.

64 Schrof, W., Rozouvan, S., Hartmann, T., Mohwald, H., Belov, V., and Van Keuren, E. (1998) Nonlinear optical properties of novel low-bandgap polythiophenes. *J. Opt. Soc. Am. B*, **15**, 889–894.

65 You, W., Cao, S., Hou, Z., and Yu, L. (2003) Fully functionalized photorefractive polymer with infrared sensitivity based on novel chromophores. *Macromolecules*, **36**, 7014–7019.

66 Yu, G., Gao, J., Hummelen, J.C., Wudl, F., and Heeger, A.J. (1995) Polymer photovoltaic cells: enhanced efficiencies via a network of internal donor–acceptor heterojuntions. *Science*, **270**, 1789–1791.

67 Wienk, M.M., Kroon, J.M., Verhees, W.J., Knol, J., Hummelen, J.C., van Hal, P.A., and Janssen, R.A. (2003) Efficient methano[70]fullerene/MDMO-PPV bulk heterojunction photovoltaic cells. *Angew. Chem. Int. Ed.*, **42**, 3371–3375.

68 Schilinsky, P., Waldauf, C., and Brabec, C.J. (2002) Recombination and loss analysis in polythiophene based bulk heterojunction photodetectors. *Appl. Phys. Lett.*, **81**, 3885.

69 Guo, X., Cui, C., Zhang, M., Huo, L., Huang, Y., Hou, J., and Li, Y. (2012) High efficiency polymer solar cells based on poly(3-hexylthiophene)/indene-C70 bisadduct with solvent additive. *Energy Environ. Sci.*, **5**, 7943.

70 McCullough, R.D. and Lowe, R.D. (1992) Enhanced electrical conductivity in regioselectively synthesized poly(3-alkylthiophenes). *J. Chem. Soc., Chem. Commun.*, 70–72.

71 Hou, J., Chen, T.L., Zhang, S., Huo, L., Sista, S., and Yang, Y. (2009) An easy and effective method to modulate molecular energy level of poly(3-alkylthiophene) for high-VocPolymer solar cells. *Macromolecules*, **42**, 9217–9219.

72 Zhou, H., Yang, L., and You, W. (2012) Rational design of high performance conjugated polymers for organic solar cells. *Macromolecules*, **45**, 607–632.

73 Cabanetos, C., El Labban, A., Bartelt, J.A., Douglas, J.D., Mateker, W.R., Frechet, J.M., McGehee, M.D., and Beaujuge, P.M. (2013) Linear side chains in benzo[1,2-b:4,5-b']dithiophene-thieno[3,4-c]pyrrole-4,6-dione polymers direct self-assembly and solar cell performance. *J. Am. Chem. Soc.*, **135**, 4656–4659.

74 Liang, Y., Xu, Z., Xia, J., Tsai, S.-T., Wu, Y., Li, G., Ray, C., and Yu, L. (2010) For the bright future—bulk heterojunction polymer solar cells with power conversion efficiency of 7.4%. *Adv. Mater.*, **22**, E135–E138.

75 Bredas, J.-L., Norton, J.E., Cornil, J., and Coropceanu, V. (2009) Molecular understanding of organic solar cells: the challenges. *Acc. Chem. Res.*, **42**, 1691–1699.

76 Liu, B., Chen, X.W., Zou, Y.P., Xiao, L., Xu, X.J., He, Y.H., Li, L.D., and Li, Y.F. (2012) Benzo[1,2-b:4,5-b']difuran-based donor–acceptor copolymers for polymer solar cells. *Macromolecules*, **45**, 6898–6905.

77 Liang, Y., Feng, D., Wu, Y., Tsai, S.-T., Li, G., Ray, C., and Yu, L. (2009) Highly efficient solar cell polymers developed via fine-tuning of structural and electronic properties. *J. Am. Chem. Soc.*, **131**, 7792–7799.

78 Chen, H.-Y., Hou, J., Zhang, S., Liang, Y., Yang, G., Yang, Y., Yu, L., Wu, Y., and Li, G. (2009) Polymer solar cells with enhanced open-circuit voltage and efficiency. *Nat. Photonics*, **3**, 649–653.

79 He, Z., Zhong, C., Su, S., Xu, M., Wu, H., and Cao, Y. (2012) Enhanced power-conversion efficiency in polymer solar cells using an inverted device structure. *Nat. Photonics*, **6**, 591–595.

80 Son, H.J., Wang, W., Xu, T., Liang, Y., Wu, Y., Li, G., and Yu, L. (2011) Synthesis of fluorinated polythienothiophene-co-benzodithiophenes and effect of fluorination on the photovoltaic properties. *J. Am. Chem. Soc.*, **133**, 1885–1894.

81 Yu, L., Liang, Y., and He, F. (2013) Semiconducting polymers. Patent WO2013116643A1.

82 Ye, L., Zhang, S., Huo, L., Zhang, M., and Hou, J. (2014) Molecular design toward highly efficient photovoltaic polymers based on two-dimensional conjugated benzodithiophene. *Acc. Chem. Res.*, **47**, 1595–1603.

83 He, Z., Xiao, B., Liu, F., Wu, H., Yang, Y., Xiao, S., Wang, C., Russell, T.P., and Cao, Y. (2015) Single-junction polymer solar cells with high efficiency and photovoltage. *Nat. Photonics*, **9**, 174–179.

84 Piliego, C., Holcombe, T.W., Douglas, J.D., Woo, C.H., Beaujuge, P.M., and Frechet, J.M. (2010) Synthetic control of structural order in N-alkylthieno[3,4-c]pyrrole-4,6-dione-based polymers for efficient solar cells. *J. Am. Chem. Soc.*, **132**, 7595–7597.

85 Zhang, Y., Hau, S.K., Yip, H.-L., Sun, Y., Acton, O., and Jen, A.K.Y. (2010) Efficient polymer solar cells based on the copolymers of benzodithiophene and thienopyrroledione. *Chem. Mater.*, **22**, 2696–2698.

86 Zou, Y., Najari, A., Berrouard, P., Beaupre, S., and Leclerc, M. (2010) A thieno[3,4-c]pyrrole-4,6-dione-based copolymer for efficient solar cells. *J. Am. Chem. Soc.*, **132**, 5330–5331.

87 Stuart, A.C., Tumbleston, J.R., Zhou, H., Li, W., Liu, S., Ade, H., and You, W. (2013) Fluorine substituents reduce charge recombination and drive structure and morphology development in polymer solar cells. *J. Am. Chem. Soc.*, **135**, 1806–1815.

88 Price, S.C., Stuart, A.C., Yang, L., Zhou, H., and You, W. (2011) Fluorine substituted conjugated polymer of medium band gap yields 7% efficiency in polymer-fullerene solar cells. *J. Am. Chem. Soc.*, **133**, 4625–4631.

89 Dou, L., Chang, W.H., Gao, J., Chen, C.C., You, J., and Yang, Y. (2013) A selenium-substituted low-bandgap polymer with versatile photovoltaic applications. *Adv. Mater.*, **25**, 825–831.

90 You, J., Dou, L., Yoshimura, K., Kato, T., Ohya, K., Moriarty, T., Emery, K., Chen, C.C., Gao, J., Li, G., and Yang, Y. (2013) A polymer tandem solar cell with 10.6% power conversion efficiency. *Nat. Commun.*, **4**, 1446.

91 Zhu, Z., Waller, D., Gaudiana, R., Morana, M., Mühlbacher, D., Scharber, M., and Brabec, C. (2007) Panchromatic conjugated polymers containing alternating donor/acceptor units for photovoltaic applications. *Macromolecules*, **40**, 1981–1986.

92 Albrecht, S., Janietz, S., Schindler, W., Frisch, J., Kurpiers, J., Kniepert, J., Inal, S., Pingel, P., Fostiropoulos, K., Koch, N., and Neher, D. (2012) Fluorinated copolymer PCPDTBT with enhanced open-circuit voltage and reduced recombination for highly efficient polymer solar cells. *J. Am. Chem. Soc.*, **134**, 14932–14944.

93 Amb, C.M., Chen, S., Graham, K.R., Subbiah, J., Small, C.E., So, F., and Reynolds, J.R. (2011) Dithienogermole as a fused electron donor in bulk heterojunction solar cells. *J. Am. Chem. Soc.*, **133**, 10062–10065.

94 Chu, T.Y., Lu, J., Beaupre, S., Zhang, Y., Pouliot, J.R., Wakim, S., Zhou, J., Leclerc, M., Li, Z., Ding, J., and Tao, Y. (2011) Bulk heterojunction solar cells using thieno[3,4-c]pyrrole-4,6-dione and dithieno[3,2-b:2′,3′-d]silole copolymer with a power conversion efficiency of 7.3%. *J. Am. Chem. Soc.*, **133**, 4250–4253.

95 Small, C.E., Chen, S., Subbiah, J., Amb, C.M., Tsang, S.-W., Lai, T.-H., Reynolds, J.R., and So, F. (2011) High-efficiency inverted dithienogermole–thienopyrrolodione-based polymer solar cells. *Nat. Photonics*, **6**, 115–120.

96 Wang, E., Ma, Z., Zhang, Z., Vandewal, K., Henriksson, P., Inganas, O., Zhang, F., and Andersson, M.R. (2011) An easily accessible isoindigo-based polymer for high-performance polymer solar cells. *J. Am. Chem. Soc.*, **133**, 14244–14247.

97 Fang, L., Zhou, Y., Yao, Y.-X., Diao, Y., Lee, W.-Y., Appleton, A.L., Allen, R., Reinspach, J., Mannsfeld, S.C.B., and Bao, Z. (2013) Side-chain engineering of isoindigo-containing conjugated polymers using polystyrene for high-performance bulk heterojunction solar cells. *Chem. Mater.*, **25**, 4874–4880.

98 Liao, Q., Cao, J., Xiao, Z., Liao, J., and Ding, L. (2013) Donor–acceptor conjugated polymers based on a pentacyclic aromatic lactam acceptor unit for polymer solar cells. *Phys. Chem. Chem. Phys.*, **15**, 19990–19993.

99 Cao, J., Chen, S., Qi, Z., Xiao, Z., Wang, J., and Ding, L. (2014) An efficient selenophene-containing conjugated copolymer for organic solar cells. *RSC Adv.*, **4**, 5085.

100 Li, H., Cao, J., Zhou, Q., Ding, L., and Wang, J. (2015) High-performance inverted PThTPTI:PC71BM solar cells. *Nano Energy*, **15**, 125–134.

101 Cao, J., Zuo, C., Du, B., Qiu, X., and Ding, L. (2015) Hexacyclic lactam building blocks for highly efficient polymer solar cells. *Chem. Commun. (Camb.)*, **51**, 12122–12125.

102 Cao, J., Qian, L., Lu, F., Zhang, J., Feng, Y., Qiu, X., Yip, H.L., and Ding, L. (2015) A lactam building block for efficient polymer solar cells. *Chem. Commun. (Camb.)*, **51**, 11830–11833.

103 Bundgaard, E. and Krebs, F.C. (2006) Low-band-gap conjugated polymers based on thiophene, benzothiadiazole, and benzobis(thiadiazole). *Macromolecules*, **39**, 2823–2831.

104 Cao, Y., Lei, T., Yuan, J., Wang, J.-Y., and Pei, J. (2013) Dithiazolyl-benzothiadiazole-containing polymer acceptors: synthesis, characterization, and all-polymer solar cells. *Polym. Chem.*, **4**, 5228.

105 Zhan, X., Tan, Z., Domercq, B., An, Z., Zhang, X., Barlow, S., Li, Y., Zhu, D., Kippelen, B., and Marder, S.R. (2007) A high-mobility electron-transport polymer with broad absorption and its use in field-effect transistors and all-polymer solar cells. *J. Am. Chem. Soc.*, **129**, 7246–7247.

106 Cheng, P., Ye, L., Zhao, X., Hou, J., Li, Y., and Zhan, X. (2014) Binary additives synergistically boost the efficiency of all-polymer solar cells up to 3.45%. *Energy Environ. Sci.*, **7**, 1351–1356.

107 Yan, H., Chen, Z., Zheng, Y., Newman, C., Quinn, J.R., Dotz, F., Kastler, M., and Facchetti, A. (2009) A high-mobility electron-transporting polymer for printed transistors. *Nature*, **457**, 679–686.

108 Kang, H., Kim, K.-H., Choi, J., Lee, C., and Kim, B.J. (2014) High-performance all-polymer solar cells based on face-on stacked polymer blends with low interfacial tension. *ACS Macro Lett.*, **3**, 1009–1014.

109 Mori, D., Benten, H., Okada, I., Ohkita, H., and Ito, S. (2014) Highly efficient charge-carrier generation and collection in polymer/polymer blend solar cells with a power conversion efficiency of 5.7%. *Energy Environ. Sci.*, **7**, 2939.

110 Earmme, T., Hwang, Y.J., Murari, N.M., Subramaniyan, S., and Jenekhe, S.A. (2013) All-polymer solar cells with 3.3% efficiency based on naphthalene diimide-selenophene copolymer acceptor. *J. Am. Chem. Soc.*, **135**, 14960–14963.

111 Earmme, T., Hwang, Y.J., Subramaniyan, S., and Jenekhe, S.A. (2014) All-polymer bulk heterojuction solar cells with 4.8% efficiency achieved by solution processing from a co-solvent. *Adv. Mater.*, **26**, 6080–6085.

112 Hwang, Y.J., Courtright, B.A., Ferreira, A.S., Tolbert, S.H., and Jenekhe, S.A. (2015) 7.7% efficient all-polymer solar cells. *Adv. Mater.*, **27**, 4578–4584.

113 Li, H., Kim, F.S., Ren, G., and Jenekhe, S.A. (2013) High-mobility n-type conjugated polymers based on electron-deficient tetraazabenzodifluoranthene diimide for organic electronics. *J. Am. Chem. Soc.*, **135**, 14920–14923.

114 Li, H., Hwang, Y.-J., Earmme, T., Huber, R.C., Courtright, B.A.E., O'Brien, C., Tolbert, S.H., and Jenekhe, S.A. (2015) Polymer/polymer blend solar cells using tetraazabenzodifluoranthene diimide conjugated polymers as electron acceptors. *Macromolecules*, **48**, 1759–1766.

115 Li, H., Earmme, T., Ren, G., Saeki, A., Yoshikawa, S., Murari, N.M., Subramaniyan, S., Crane, M.J., Seki, S., and Jenekhe, S.A. (2014) Beyond fullerenes: design of nonfullerene acceptors for efficient organic photovoltaics. *J. Am. Chem. Soc.*, **136**, 14589–14597.

116 Li, H., Hwang, Y.J., Courtright, B.A., Eberle, F.N., Subramaniyan, S., and Jenekhe, S.A. (2015) Fine-tuning the 3D structure of nonfullerene electron acceptors toward high-performance polymer solar cells. *Adv. Mater.*, **27**, 3266–3272.

117 Li, J., Zhao, Y., Tan, H.S., Guo, Y., Di, C.A., Yu, G., Liu, Y., Lin, M., Lim, S.H., Zhou, Y., Su, H., and Ong, B.S. (2012) A stable solution-processed polymer semiconductor with record high-mobility for printed transistors. *Sci. Rep.*, **2**, 754.

118 Sirringhaus, H., Brown, P.J., Friend, R.H., Nielsen, M.M., Bechgaard, K., Langeveld-Voss, B.M.W., Spiering, A.J.H., Janssen, R.A.J., Meijer, E.W., Herwig, P., and de Leeuw, D.M. (1999) Two-dimensional charge transport in self-organized, high-mobility conjugated polymers. *Nature*, **401**, 685–688.

119 McCulloch, I., Heeney, M., Bailey, C., Genevicius, K., Macdonald, I., Shkunov, M., Sparrowe, D., Tierney, S., Wagner, R., Zhang, W., Chabinyc, M.L., Kline, R.J., McGehee, M.D., and Toney, M.F. (2006) Liquid-crystalline semiconducting polymers with high charge-carrier mobility. *Nat. Mater.*, **5**, 328–333.

120 Kim, J., Lim, B., Baeg, K.-J., Noh, Y.-Y., Khim, D., Jeong, H.-G., Yun, J.-M., and Kim, D.-Y. (2011) Highly soluble poly(thienylenevinylene) derivatives with charge-carrier mobility exceeding $1 \, \text{cm}^2 \, \text{V}^{-1} \, \text{s}^{-1}$. *Chem. Mater.*, **23**, 4663–4665.

121 Lei, T., Cao, Y., Fan, Y., Liu, C.J., Yuan, S.C., and Pei, J. (2011) High-performance air-stable organic field-effect transistors: isoindigo-based conjugated polymers. *J. Am. Chem. Soc.*, **133**, 6099–6101.

122 Lei, T., Dou, J.H., and Pei, J. (2012) Influence of alkyl chain branching positions on the hole mobilities of polymer thin-film transistors. *Adv. Mater.*, **24**, 6457–6461.

123 Mei, J., Kim, D.H., Ayzner, A.L., Toney, M.F., and Bao, Z. (2011) Siloxane-terminated solubilizing side chains: bringing conjugated polymer backbones closer and boosting hole mobilities in thin-film transistors. *J. Am. Chem. Soc.*, **133**, 20130–20133.

124 Schwartz, G., Tee, B.C., Mei, J., Appleton, A.L., Kim, D.H., Wang, H., and Bao, Z. (2013) Flexible polymer transistors with high pressure sensitivity for application in electronic skin and health monitoring. *Nat. Commun.*, **4**, 1859.

125 Lee, J., Han, A.R., Kim, J., Kim, Y., Oh, J.H., and Yang, C. (2012) Solution-processable ambipolar diketopyrrolopyrrole-selenophene polymer with unprecedentedly high hole and electron mobilities. *J. Am. Chem. Soc.*, **134**, 20713–20721.

126 Lee, J., Han, A.R., Yu, H., Shin, T.J., Yang, C., and Oh, J.H. (2013) Boosting the ambipolar performance of solution-processable polymer semiconductors via hybrid side-chain engineering. *J. Am. Chem. Soc.*, **135**, 9540–9547.

127 Chen, H., Guo, Y., Yu, G., Zhao, Y., Zhang, J., Gao, D., Liu, H., and Liu, Y. (2012) Highly pi-extended copolymers with diketopyrrolopyrrole moieties for high-performance field-effect transistors. *Adv. Mater.*, **24**, 4618–4622.

128 Grimsdale, A.C., Chan, K.L., Martin, R.E., Jokisz, P.G., and Holmes, A.B. (2009) Synthesis of light-emitting conjugated polymers for applications in electroluminescent devices. *Chem. Rev.*, **109**, 897–1091.

129 Ma, H., Yip, H.-L., Huang, F., and Jen, A.K.Y. (2010) Interface engineering for organic electronics. *Adv. Funct. Mater.*, **20**, 1371–1388.

130 Burroughes, J.H., Bradley, D.D.C., Brown, A.R., Marks, R.N., Mackay, K., Friend, R.H., Burns, P.L., and Holmes, A.B. (1990) Light-emitting diodes based on conjugated polymers. *Nature*, **347**, 539–541.

131 Bubudri, F., Cicco, S.R., Farinola, G.M., and Naso, F. (1996) Synthesis, characterization and properties of a soluble polymer with a poly(phenyleneviny1ene) structure. *Macromol. Rapid Commun.*, **17**, 905–911.

132 Li, X., Zhang, Y., Yang, R., Huang, J., Yang, W., and Cao, Y. (2005) Novel saturated red-emitting poly(p-phenylenevinylene) copolymers with narrow-band-gap units of 2,1,3-benzothiadiazole synthesized by a palladium-catalyzed Stille coupling reaction. *J. Polym. Sci., Part A: Polym. Chem.*, **43**, 2325–2336.

133 Li, X., Zeng, W., Zhang, Y., Hou, Q., Yang, W., and Cao, Y. (2005) Synthesis and properties of novel poly(p-phenylenevinylene) copolymers for near-infrared emitting diodes. *Eur. Polym. J.*, **41**, 2923–2933.

134 Tian, J., Wu, C.-C., Thompson, M.E., Sturm, J.C., and Registers, R.A. (1995) Photophysical properties, self-assembled thin films, and light-emitting diodes of poly(p-pyridylviny1ene)s and poly(p-pyridinium viny1ene)s. *Chem. Mater.*, **7**, 2190–2198.

135 Onoda, M. (1995) Light-emitting diodes using n-type conducting polymer: poly(p-pyridyl vinylene). *J. Appl. Phys.*, **78**, 1327.

136 Mausella, M.J., Fu, D.-K., and Swager, T.M. (1995) Synthesis of regioregular poly(methyl pyridinium vinylene): an isoelectronic analogue to poly(phenylene vinylene). *Adv. Mater.*, **7**, 145–147.

137 Lere-Porte, J.-P., Moreau, J.J.E., and Torreilles, C. (2001) Highly conjugated poly(thiophene)s – Synthesis of regioregular 3-alkylthiophene polymers and 3-alkylthiophene/thiophene copolymers. *Eur. J. Org. Chem.*, **2001**, 1249–1258.

138 Melucci, M., Favaretto, L., Barbarella, G., Zanelli, A., Camaioni, N., Mazzeo, M., and Gigli, G. (2007) Synthesis and optoelectronic properties of a red emitting branched polymer containing V-shaped oligothiophene-S,S-dioxides as repeating units. *Tetrahedron*, **63**, 11386–11390.

139 Ohshita, J., Kimura, K., Lee, K.-H., Kunai, A., Kwak, Y.-W., Son, E.-C., and Kunugi, Y. (2007) Synthesis of silicon-bridged polythiophene derivatives and their applications to EL device materials. *J. Polym. Sci., Part A: Polym. Chem.*, **45**, 4588–4596.

140 Mishra, S.P., Palai, A.K., Srivastava, R., Kamalasanan, M.N., and Patri, M. (2009) Dithieno[3,2-b:2′,3′-d]pyrrole-alkylthiophene-benzo[c][1,2,5]thiadiazole-based highly stable and low band gap polymers for polymer light-emitting diodes. *J. Polym. Sci., Part A: Polym. Chem.*, **47**, 6514–6525.

141 Emge, A. and Bauerle, P. (1999) Molecular recognition properties of nucleobase-functionalized polythiophenes. *Synth. Met.*, **102**, 1370–1373.

142 Bauerle, P. and Emge, A. (1998) Specific recognition of nucleobase-functionalized polythiophenes. *Adv. Mater.*, **3**, 324–330.

143 McQuade, D.T., Pullen, A.E., and Swager, T.M. (2000) Conjugated polymer-based chemical sensors. *Chem. Rev.*, **100**, 2537–2574.

144 Marsella, M.J., Carroll, P.J., and Swager, T.M. (1995) Design of chemoresistive sensory materials: polythiophene-based pseudopolyrotaxanes. *J. Am. Chem. Soc.*, **117**, 9832–9841.

145 Kawabata, K. and Goto, H. (2009) Liquid crystalline π-conjugated copolymers bearing a pyrimidine type mesogenic group. *Materials*, **2**, 22–37.

146 Ho, C.-L. and Wong, W.-Y. (2011) Metal-containing polymers: facile tuning of photophysical traits and emerging applications in organic electronics and photonics. *Coord. Chem. Rev.*, **255**, 2469–2502.

147 Nicolaou, K.C., Chakraborty, T.K., Piscopio, A.D., Minowa, N., and Bertinato, P. (1993) Total synthesis of rapamycin. *J. Am. Chem. Soc.*, **115**, 4419–4420.

148 Shair, M.D., Yoon, T., and Danishefsky, S.J. (1994) A remarkable cross coupling reaction to construct the endyne linkage relevant to dynemicin A: synthesis of the deprotected ABC system. *J. Org. Chem.*, **59**, 3755–3757.

149 Yamamoto, T., Sanechika, K., and Yamamoto, A. (1980) Preparation of thermalstable and electric-conducting poly(2,5-thienylene). *J. Polym. Sci.: Polym. Lett. Ed.*, **18**, 9–12.

150 Gallagher, W.P., Terstiege, I., and Maleczka, R.E. (2001) Stille couplings catalytic in tin: the "Sn−O" approach. *J. Am. Chem. Soc.*, **123**, 3194–3204.

151 Gallagher, W.P. and Maleczka, R.E.J. (2005) Stille reactions catalytic in tin: a "Sn-F" route for intermolecular and intramolecular couplings. *J. Org. Chem.*, **70**, 841–846.

152 Louaisil, N., Pham, P.D., Boeda, F., Faye, D., Castanet, A.-S., and Legoupy, S. (2011) Ionic liquid supported organotin reagents: green tools for Stille cross-coupling reactions with brominated substrates. *Eur. J. Org. Chem.*, **2011**, 143–149.

153 Lu, L., Zheng, T., Xu, T., Zhao, D., and Yu, L. (2015) Mechanistic studies of effect of dispersity on the photovoltaic performance of PTB7 polymer solar cells. *Chem. Mater.*, **27**, 537–543.